NASA Technical Paper 2985

AVSCOM Technical Report 89-C-008

1990

Computer Code for Predicting Coolant Flow and Heat Transfer in Turbomachinery

Peter L. Meitner
Propulsion Directorate
USAARTA-AVSCOM
Lewis Research Center
Cleveland, Ohio

National Aeronautics and Space Administration
Office of Management
Scientific and Technical Information Division

Summary

The computer program Coolant Passage Flow (CPF) was developed specifically for radial turbomachinery but can be used to analyze any turbomachinery coolant flow path geometry that consists of a single flow passage with a single inlet and exit. Flow can be bled off for tip-cap impingement cooling, and a flow bypass can be specified in which coolant flow is taken off at one point in the flow channel and reintroduced at a point farther downstream in the same channel. The user may either choose the coolant flow rate or let the program determine the flow rate from specified inlet and exit conditions. The main coolant flow must be subsonic everywhere except at the exit, where choked flow is allowed. Choked flow is also allowed at the bypass exit and at the tip-cap inlet and exit.

CPF integrates the one-dimensional momentum and energy equations along a defined flow path and calculates the coolant's flow rate, temperature, pressure, and velocity and the heat transfer coefficients along the passage. The equations account for area change, mass addition or subtraction, pumping, friction, and heat transfer.

The flow path geometry is described in Cartesian coordinates at node points that, in turn, divide the flow path into a desired number of intervals. Each interval may be further subdivided into any desired number of slices to increase calculation accuracy. Standard correlations are used to predict the frictional pressure drop and the heat transfer coefficient for each interval, which is specified as being either a plain, a pin-finned, a trip-strip, or a finned passage. Alternatively, the friction factors and the heat transfer coefficients for each interval may be either specified directly or input as curves in tabular form.

This report presents a detailed description of the program input and output, including error messages. Three example problems illustrate the use of the code, demonstrate the calculation accuracy as a function of the change in free flow area between nodes, and show a comparison with Fanno and Rayleigh line predictions. The report also presents all the analysis equations, as well as the derivations of the one-dimensional momentum and energy equations.

Introduction

In small turbomachinery the radial turbine has several inherent advantages over an axial turbine. Among these are higher overall work extraction, greater aerodynamic efficiency, and less sensitivity to tip clearance. These attributes have resulted in the widespread use of uncooled radial turbines in automotive turbochargers and auxiliary power units, but their use in primary powerplants (where higher operating temperatures and pressures are desired) has been held back by the difficulty of fabricating a cooled radial turbine. Both the U.S. Army and NASA, in a series of contractual efforts (refs. 1 to 4), have investigated techniques for fabricating cooled radial turbines. These efforts, although contributing significantly to solving the manufacturing problems, focused relatively little effort on the internal heat transfer of cooled radial turbines. The internal heat transfer calculations were performed, for the most part, by using company proprietary flow codes, along with approximations based on axial turbine experience. When NASA and the Army Propulsion Directorate decided to design an in-house cooled radial turbine for possible evaluation in the new Small Warm Turbine Facility, a computer code had to be developed that would accurately predict coolant flow and heat transfer inside cooled turbomachinery. The computer code Coolant Passage Flow (CPF) described in this report is the result of that effort.

Although specifically developed for radial turbomachinery, CPF can be used to analyze any turbomachinery coolant flow geometry that consists of a single flow passage with a single inlet and exit. CPF integrates the one-dimensional momentum and energy equations along a defined flow path and calculates the coolant's flow rate, temperature, pressure, and velocity and the heat transfer coefficients along the passage. The equations account for area change, mass addition or subtraction, pumping (radius change), friction, and heat addition. Flow can be bled off for tip-cap impingement cooling, and a flow bypass can be specified in which coolant flow is taken off at one point in the flow channel and reintroduced at a point farther downstream in the same channel. The user may either choose the coolant flow rate or let the program calculate the flow rate from specified inlet and exit conditions.

This report describes the program's input, output, and error messages and illustrates the use of the code by three example cases. All the analysis equations are shown, along with their derivations and necessary assumptions where appropriate. An added feature of CPF that allows direct specification of heat generation in a given flow interval is described in appendix E, written by Teresa R. Kline. A heat generation term has been added to the energy equation. This feature allows the direct solution of the Rayleigh line problem (see example

problem 3). CPF can be obtained from the Computer Software Management Information Center (COSMIC), University of Georgia, Athens, Georgia, 30602.

Flow Path Modeling

A composite sketch of the types of flow and heat transfer configurations that can be analyzed with CPF is shown in figure 1. CPF determines the coolant's flow rate, temperature, pressure, and velocity and the heat transfer coefficients along any arbitrary passage with a single inlet and exit. Note that internal flow division is not allowed, except for the shown tip-cap impingement flow and bypass flow. Bypass flow is taken off at one point in the flow channel and reintroduced at a point farther downstream in the same channel. The three flow channels shown in figure 1 would thus be analyzed separately. The calculation frame of reference is the rotating frame (moving with the turbomachinery). Thus, when the rotational speed is greater than zero, all coolant input and output total pressures and temperatures are relative total conditions.

The flow path is defined with the Cartesian coordinates z, r, and y as shown in figure 1, where z is the axial direction and the axis of rotation, r is the radial direction, and y is perpendicular to both z and r. (All symbols are defined in appendix A.) The flow path geometry is described at nodes (at the passage centroid) that, in turn, determine a specified number of intervals (input parameter NI). The nodes and intervals for the example 1 upper flow path are shown in figure 2. Along the flow path, the n^{th} interval is that flow path length immediately preceding node n. Note that the inlet is specified separately and that the last (NI^{th}) node is the exit. Also note that several nodes are coincident. These coincident nodes result from specifying zero-length "fake" intervals. These intervals, along with all input variables, are fully described in the section Program Input.

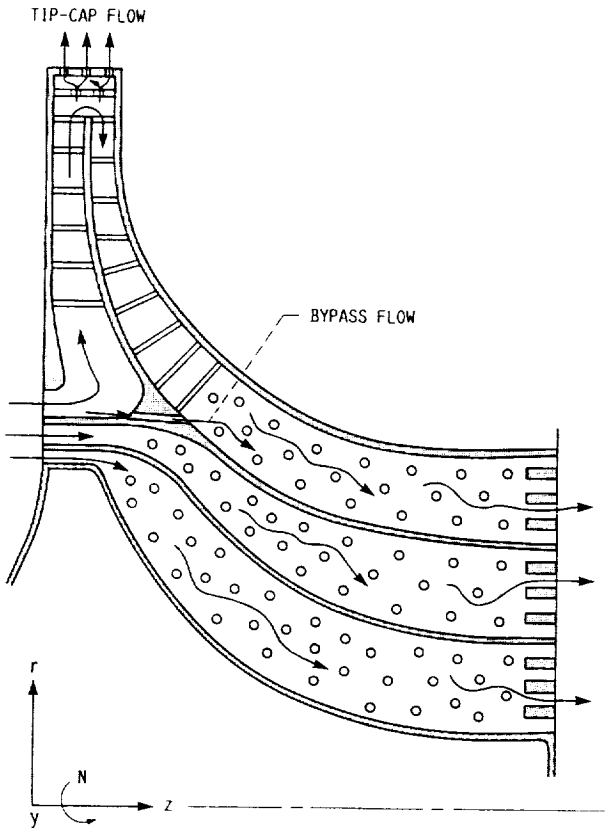

Figure 1.—Conceptual cooled radial turbine configuration.

Flow path geometry variables consisting of node location, free flow area, and hydraulic diameter are specified at each node. Standard correlations are used to predict the frictional pressure drop and the heat transfer coefficient for each interval, which is specified as being either a plain, a pin-finned, a trip-strip, or a finned passage. Alternatively, the friction factors and the heat transfer coefficients for each interval may be either specified directly or input as curves in tabular form. Each interval must be designated either a regular or a fake interval. Sudden step changes in flow area are modeled via fake intervals, in which the total pressure drop is calculated from established correlations.

The change in free flow area between nodes defining a regular interval has a strong influence on the accuracy of the flow calculations. This means that, for geometries with significant area change, the nodes should be spaced close together but, for geometries with small area change, the nodes may be spaced farther apart. In order to avoid having to input an excessive number of nodes, an option can be used that divides each input interval (the interval that lies between input nodes) into a specified number of slices to get a more accurate flow solution. The program then switches from the input nodal frame of reference (shown in fig. 2) to the new, slice frame of reference, and new node and new interval numbers are

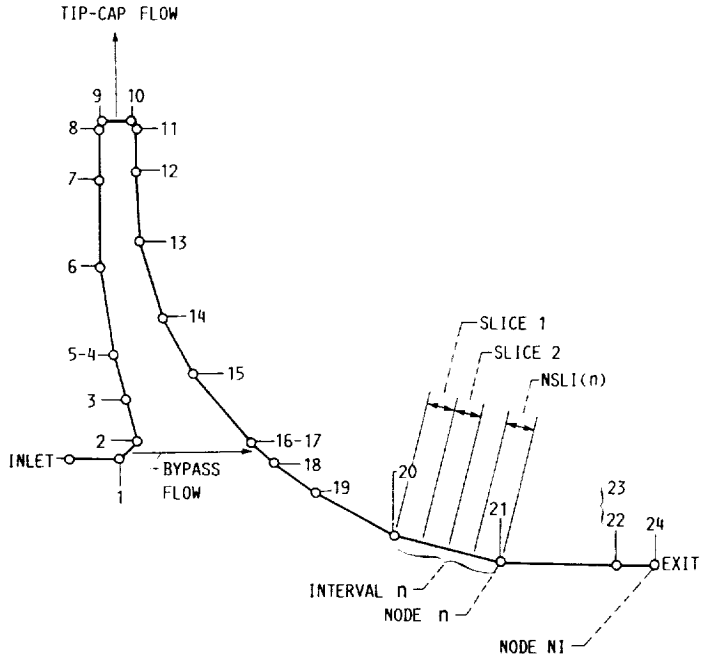

Figure 2.—Nodal representation of figure 1 upper flow path.

created in accordance with the total number of slices. All calculations are then performed in the new frame of reference. The required node parameters needed at the new node (slice) locations are obtained by linear interpolation of the appropriate original input nodal values. Input variables that were specified for the original input intervals are retained for the new intervals (which were created by slicing up the original intervals). For additional calculation accuracy, the program further divides all intervals (either the original input intervals or the calculated intervals generated by the slice option) into smaller sections called steps. The flow solution is marched along these steps from node to node and iteratively converged on the flow Mach number. The iterative flow solution procedure is described in detail in appendix B.

Output may be specified in the original frame of reference or in the new, slice frame of reference. The total number of slices allowed has arbitrarily been set at 250. This can be increased to any desired number by changing the DIMENSION statements at the beginning of the code. Example 2 (see the section Example Problems) illustrates the calculation accuracy achieved for various rates of free flow area change between nodes.

The user may either choose the coolant flow rate or let the program determine the flow rate from specified inlet and exit conditions. The coolant flow must be subsonic at all internal flow path nodes. Choked (sonic) flow is allowed only at the exit node, the bypass exit, and the tip-cap inlet and exit. If the coolant flow is calculated from specified inlet and exit pressures and supersonic flow is calculated at internal flow path nodes, the weight flow is reduced to achieve subsonic flow. If a weight flow is specified and that flow is too large for the flow geometry, the program terminates with an appropriate error message.

Program Input

The program input parameters are listed in appendix C, along with the parameter description, the required units, the type of variable (real or integer), and the default values. Except for the title, all data input is in NAMELIST format. Although the appendix is essentially self-explanatory, the following matters and variables require further discussion.

Input Curves

Various parameters may be specified as curves in tabular form. Each table is described by five input parameters: an integer variable describing the number of points in the table, two subscripted parameters corresponding to the curve x and y values, and two parameters that specify the type of x and y axes (Cartesian or logarithmic (base 10)). Subroutine SPLFIT generates a spline curve fit from the tabular input. Each curve must be described by a minimum of 3 to a maximum of 25 points, with the abscissa (x axis) values input in ascending order. The slopes at the curve end points are evaluated from the first two and last two data points. These points must thus be selected to give a good representation of the curve slope at each end.

Flow Angles

Figure 3 is a schematic of the angle definitions for generalized bypass and impingement flows. At present the angle inputs ALIMP and ALBPI are dummy variables that have no effect on any calculations. They have been included for anticipated future uses as explained in the description of those variables.

Nonsubscripted Variables

Title.—The title input may be up to 80 alphanumeric characters in length. It is the overall title for each job submission and does not get input repeatedly if successive cases are run in a single data stack. The title is, however, printed out for each case in a data stack.

IOPPRP.—If the physical properties specification is set equal to 0, the user inputs the coolant's specific heat ratio, specific heat, viscosity, and thermal conductivity. These values are then assumed to remain constant for all flow calculations. If IOPPRP is set equal to 1, the coolant's physical properties are evaluated from the subroutine AIRPRP. The properties vary and are calculated at local static temperatures.

PTSP and TTSP.—The inlet supply total pressure and total temperature must be specified in the relative frame of reference (relative total conditions) if the rotational speed (input parameter RPM) is greater than 0. For no rotation these variables are specified in the absolute frame of reference.

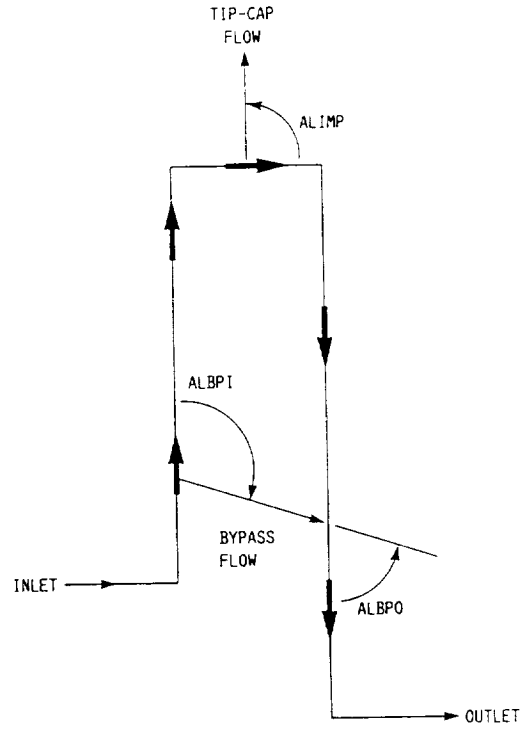

Figure 3.—Angle definitions for generalized flow path.

KTIN.—The inlet total pressure loss coefficient accounts for various inlet configurations and can assume a value between 0.0 and 1.0. If it is equal to 0.0, the inlet total pressure is set equal to the specified supply total pressure (PTSP); if it is equal to 1.0, the inlet total pressure loses one full velocity head.

Nodal or Interval Variables

Geometry parameters or geometry and flow and heat transfer parameters must be supplied at the input nodal points and for the intervals defined by these nodal points. For the nodal or interval subscripted parameters of appendix C (identified as variable type R(NI) or I(NI)), only the variables Z, R, Y, A, and DH are nodal values, in that they define values at each input node location. All other variables are interval values and represent average values over the interval. The nodal values in appendix C are identified by the superscript *nd*, and the interval values by the superscript *i*.

For each nodal or interval input parameter, an array of NI numbers must be specified, even though actual values may be needed for only a few nodes or intervals. The values that are not needed are thus dummy or fill-in values, but they must still be specified. For example, if a flow path consists of 20 intervals and the user wishes to let the program calculate the friction factors in the first 10 intervals but wants to specify the friction factors in the last 10 intervals (via the parameter F), the first 10 numbers of the 20-number F array are dummy values, and only the last 10 numbers are used by the code.

***NSLI*(n).**—For large area variations between nodes the calculation procedure introduces small artificial increases or decreases in calculated total pressure and total temperature (see example 2 in the section Example Problems). This parameter specifies the number of slices into which each interval is to be divided in order to increase the accuracy of the calculation procedure. For certain intervals, only one slice (no dividing) is allowed, and no matter what values of NSLI(n) are input, the program defaults NSLI(n) to 1. These intervals are (1) fake intervals; (2) tip-cap flow intervals; (3) bypass intervals (flow leaving and entering); and (4) intervals in which a total pressure loss coefficient (K factor; K_T) is specified by the input variable KTSGMT.

***IOPTFI*(n).**—This parameter designates fake intervals, which are used to model abrupt area changes (such as occur when there is a change in the interval heat transfer configuration). By using fake intervals the correct total pressure drop can be calculated from established correlations for sudden increases or decreases in flow area. Fake intervals may be used anywhere in the flow path and should be of zero length. That is, the coordinates of the nodes bracketing the fake interval should be identical. Example 1 (in the section Example Problems) shows how fake intervals are used between intervals with different heat transfer geometries to model the sudden area changes.

***IOPTHT*(n) *and IOPTFF*(n).**—These variables specify the types of heat transfer and friction factor calculations, respectively, for each interval. IOPTHT(n) and IOPTFF(n) are the main controlling parameters in that they determine the specific information used in each interval for the requested heat transfer and friction calculations. Only certain combinations of IOPTHT(n) and IOPTFF(n) are allowed for each interval. These combinations are shown in table I. The heat transfer coefficient may be user specified (IOPTHT(n) = 0), obtained from internal correlations (IOPTHT(n) = 1, 2, 3, or 4 for trip strips, pin fins, finned passage, and plain passage, respectively), or may be determined from an input Colburn J-factor curve (IOPTHT(n) = 5). The friction factor may also be user specified (IOPTFF(n) = 0), obtained from trip-strip geometry input (IOPTFF(n) = 1), obtained from an appropriate input curve (IOPTFF(n) = 2), obtained from a roughened-plain-passage correlation (IOPTFF(n) = 3), or obtained from a specified K factor by means of the input parameter KTSGMT (IOPTFF(n) = 4). Only the combinations of IOPTHT(n) and IOPTFF(n) shown in table I are allowed. If unallowed combinations are chosen, the program aborts and prints out an appropriate error message. For fake intervals, dummy values *must* be input for both IOPTHT(n) and IOPTFF(n).

Note that CPF does *not* check that the interval inputs are consistent with the specified values of IOPTHT(n) and IOPTFF(n). The user must thus make sure that the correct type of information is supplied for each input interval.

***FCOR*(n), *HCCOR*(n), *and HTACOR*(n).**—The user may modify values of friction factor, heat transfer coefficient, and

TABLE I.—ALLOWED COMBINATIONS OF IOPTHT AND IOPTFF

Heat transfer coefficient option, IOPTHT	Friction factor option, IOPTFF
0—User specified	0—User specified
1—Trip strips	1—Trip strips
2—Pin fins	0—User specified 2—Input curve (NPFF2, etc.)
3—Finned passage	0—User specified 2—Input curve (NPFF3, etc.) 3—Roughened-plain-passage correlation (ref. 7)
4—Plain passage (internal correlation)	0—User specified 2—Input curve (NPFF4, etc.) 3—Roughened-plain-passage correlation (ref. 7) 4—Specified K factor
5—Input Colburn J-factor curve (NPCJF, etc.)	0—User specified 2—Input curve (NPFF4, etc.) 3—Roughened-plain-passage correlation (ref. 7) 4—Specified K factor

heat transfer area by the correction factors FCOR(n), HCCOR(n), and HTACOR(n), respectively. Consider the flow path shown in figure 4, in which nodes $n - 1$ and n define a 180° bend. The program calculates the straight-line distance between the nodes. Note that the true distance between the nodes (along the flow direction) is significantly greater than the calculated distance. If the friction pressure drop is specified by the Fanning friction factor (IOPTFF(n) = 0, 1, 2, or 3), the friction factor must be modified by

$$\text{FCOR}(n) = \frac{\text{True distance}}{\text{Calculated straight-line distance}}$$

If the friction pressure drop is specified by a total pressure loss coefficient (IOPTFF(n) = 4), no correction is needed, since the loss coefficient is specified for a given geometry (e.g., a 180° bend) and thus is independent of actual flow path length. For the geometry shown in figure 4, the heat transfer area must similarly be modified by

$$\text{HTACOR}(n) = \frac{\text{True distance}}{\text{Calculated straight-line distance}}$$

The heat transfer coefficient correction factor HCCOR allows the user to account for inlet or turning effects. The use of the described modifiers allows flexibility in applying the program. Note, however, that their use cannot be hidden, since they are always shown in the program output.

***IOPTCR*(n).**—This input parameter controls the option for calculating a heat transfer coefficient correction due to rotation. If IOPTCR(n) is set equal to 0 (default value), no correction is made, and the heat transfer coefficient rotation modifier HCCORC(n) (not an input; see the section Program Output) is defaulted to 1.0. If IOPTCR(n) is set equal to 1, the calculated or specified heat transfer coefficient is modified as described in appendix B. Note that the correction is valid only for purely radial flow in plain passages and for fluid temperatures lower than the wall temperature (the fluid cooling the wall). The calculated correction factor HCCORC(n) may be greater or less than 1.0 and is shown in the program output.

***EDD*(n) *and PDE*(n).**—These parameters describe the geometry for trip strips. They are shown schematically in figure 5.

***NFNP*(n), *THFN*(n), *SPFN*(n), *and HHTFN*(n).**—These parameters describe the geometry for finned passages. They are shown schematically in figure 6.

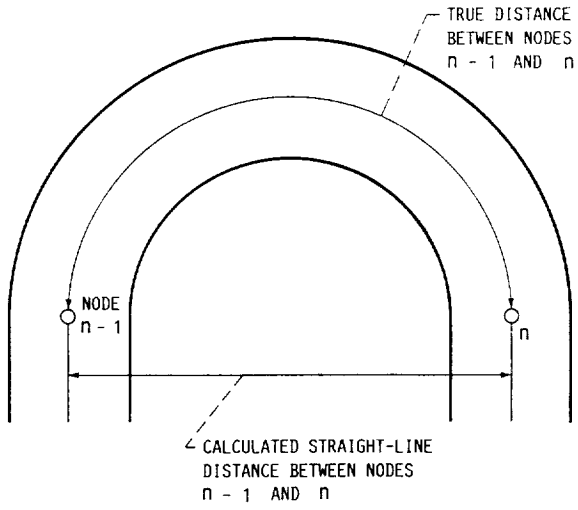

Figure 4.—Comparison of true and calculated distances in 180° bend.

INPUT PARAMETER	DEFINITION
EDD	e/D
PDE	p/e

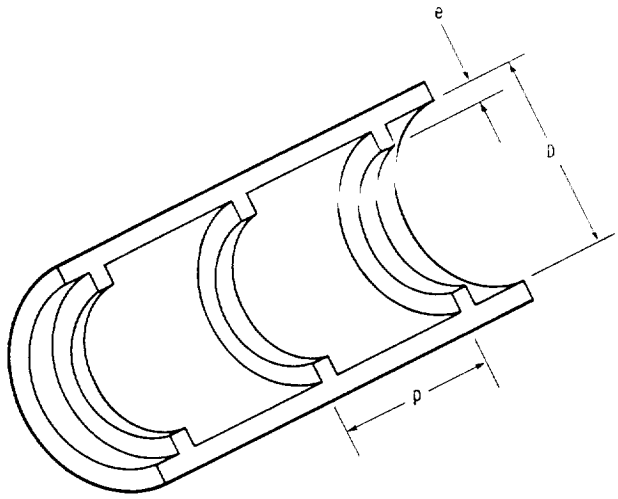

Figure 5.—Trip-strip geometry parameters.

INPUT PARAMETER	DEFINITION
THFN	τ_f
SPFN	$\tau_f + m$
HHTFN	L_f
NFNP	NUMBER OF FINNED PASSAGES

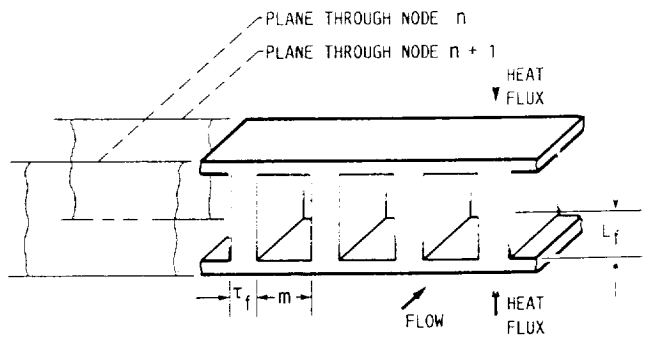

Figure 6.—Finned-passage geometry parameters.

***A*(n) *and DH*(n).**—The flow area and the hydraulic diameter based on minimum free flow area must be input for each node. These nodal values are used in evaluating the local Mach and Reynolds numbers.

***AV*(n) *and DHV*(n).**—The flow area and hydraulic diameter based on open volume are needed only for pin-fin intervals. They are required in addition to the input variables A(n) and DH(n). The interval values AV(n) and DHV(n) are used in the pin-fin heat transfer correlation. AV(n) is equal to V/ℓ, where V is the open volume in the interval and ℓ is the interval length; DHV(n) is equal to $4V/S$, where S is the total heat transfer surface area in the interval (endwall plus pin fins).

Parameters Specifying Location of Tip-Cap and Bypass Flow

The variables NTCF, NBPI, and NBPO define the interval in which a tip-cap flow, the start of a bypass channel, or the end of a bypass channel, respectively, is specified. This is illustrated in the example flow path of figure 2, where the tip-cap flow leaves from interval 10 and the bypass channel starts in interval 2 and ends in interval 18. The first interval should not be a tip-cap interval or contain the start of a bypass channel (NTCF $\neq$ 1, NBPI $\neq$ 1). Any one interval can only be assigned one of these three options. This means that a tip cap and the start of a bypass channel cannot be specified for the same interval (NTCF $\neq$ NBPI), nor can a tip cap be in the interval ending a bypass channel (NTCF $\neq$ NBPO). It is also not recommended that the last interval contain the end of the bypass channel (NBPO $\neq$ NI). Note that tip-cap or bypass flows cannot be specified for fake intervals.

Further comments are in order regarding the use of a bypass channel. Subroutine BYPSFL, which calculates the bypass flow, is a simplified version of the main routine used to calculate the coolant flow in CPF. The two main simplifications are that heat transfer is not considered for the bypass flow and that all calculations are based on constant physical properties. Both the inlet and exit conditions for the bypass channel are taken to be the average of the values at the respective interval end points. This implies that, for maximum accuracy, these intervals should be kept as short as possible. Further accuracy will be gained if these intervals are of constant cross-sectional area. Also, for best results, the bypass flow should not be a significant fraction of the main coolant flow.

Tip-Cap Parameters for Interval NTCF

The parameters that describe the geometry for tip-cap flow are shown schematically in figure 7. The impingement angle ALIMP shown in figure 3 is a dummy variable that has no effect on the calculations. It is included for possible future use in a more general impingement flow calculation procedure.

Bypass Channel Parameters

PBPRI.—This variable specifies the pressure recovery at the bypass inlet and is determined by the geometry of that

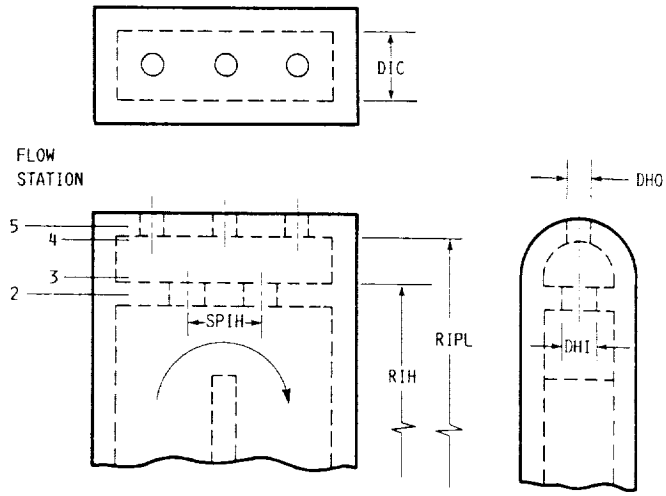

Figure 7.—Tip-cap geometry parameters and flow stations.

inlet. PBPRI must be set between 0.0 and 1.0. Setting PBPRI equal to 0.0 causes the bypass inlet total pressure to be set equal to the bypass inlet interval average *static* pressure. Such a condition exists if the bypass flow is drawn off perpendicular to the main coolant flow. Setting PBPRI equal to 1.0 causes the bypass inlet total pressure to be set equal to the bypass inlet interval average *total* pressure. Such a condition exists if the bypass flow is drawn off tangential to the main coolant flow.

ALBPI.—This angle describes the component of velocity of the bypass exiting flow in the main-stream coolant flow direction for interval NBPI. ALIBPI is a dummy variable that has no effect on any calculation. It is anticipated that in the future this variable, along with additional geometry parameters, will be used in a generalized calculation procedure for the pressure recovery at the bypass inlet.

ALBPO.—This angle describes the component of velocity of the bypass entering flow in the main-stream coolant flow direction for interval NBPO. ALBPO is equal to 0° for bypass flow entering tangential to the main-stream flow and equal to 90° for bypass flow entering perpendicular to the main-stream flow. Figure 3 shows all flow angle definitions.

Miscellaneous Comments

During the initial flow path modeling the specified free flow areas, as well as the inlet and exit pressures, may not be compatible with physically possible flow. For complex flow geometries it is suggested that the initial calculations be performed with a specified flow rate (IOPTW = 0) to make the calculations independent of exit backpressure. Starting with a low flow rate (to ensure subsonic flow at all internal nodes), the high Mach number locations can be identified and the flow areas increased, if necessary, as the flow rate is increased. Also, the calculated trailing-edge pressure can be used to size the exit area for compatibility with the backpressure.

Some care must be taken with the last interval for choked exit flow. If the flow area is constant in the last interval

```
TITLE ——— EXAMPLE PROBLEM 1 (FIGURE 1 UPPER FLOW PATH)
OVERALL PARAMETERS, INLET, AND EXIT CONDITIONS ——— &DATT RG=53.35, RPM=3.7E4, NI=24, IECHO=0, DHIN=0.2310, NSLI=24*2, ISLOUT=0,
  ZIN=0.0, RIN=3.85, YIN=0.0, AIN=.0625,
  IOPTW=1, PTSP=175., TTSP=750., KTIN=.50, POUT=50.0,
FANNING FRICTION FACTOR CURVE ——— NPFF4=12, RE4=100., 500., 1.E3, 2.E3, 2.5E3, 3.E3, 3.5E3, 4.E3, 5.E3,
  1.E4, 1.E5, 1.E6,
  FFF4=.170, .034, .017, .0085, .007, .0077, .010, .0107, .010, .008,
    .0043, .0029,
COLBURN J FACTOR CURVE ——— IXCJF=1, IYCJF=1,
  NPCJF=8, RECJF=1.E2, 1.E3, 2.E3, 3.E3, 6.E3, 1.E4, 1.E5, 1.E6,
  CJF=.044, .0045, .0023, .0026, .0032, .0029, .0019, .0013,
GEOMETRIC FLOW PATH ——— Z=0.40, 0.50, 0.44, 0.35, 0.35, 0.23, 0.20, 0.20, 0.22, 0.48, 0.50,
    0.50, 0.52, 0.72, 0.95, 1.40, 1.40, 1.63, 1.92, 2.55, 3.40, 4.30,
    4.30, 4.62, 126*0.0,
  R=3.85, 4.00, 4.35, 4.65, 4.65, 5.35, 6.02, 6.43, 6.43, 6.43, 6.43,
    6.10, 5.55, 4.95, 4.55, 4.00, 4.00, 3.85, 3.60, 3.25, 3.06, 3.03,
    3.03, 3.03, 126*0.,
  Y=15*0.0, 2*0.07, 0.10, 0.18, 0.47, 1.15, 2.35, 2.35, 2.80, 126*0.0,
OPTIONS FOR FAKE INTERVAL, HEAT TRANSFER, AND FRICTION FACTOR ——— IOPTFI=0, 0, 0, 0, 1, 0, 0, 0, 0, 0, 0, 0,
    0, 0, 0, 0, 1, 0, 0, 0, 0, 0, 1, 0, 126*0,
  IOPTHT=4*4, 7, 3*1, 4, 5, 4, 5*1, 7, 5*2, 7, 3, 126*7,
  IOPTFF=4*2, 7, 3*1, 4, 4, 4, 5*1, 7, 5*0, 7, 3, 126*7,
  EDD=150*0.145, PDE=150*10.0, DOE=150*1.E5,
  KTSGMT=8*0.0, 1.65, 1.65, 1.65, 139*0.0,
FINNED PASSAGE PARAMETERS ——— NFNP=23*0, 4, 126*0,
  THFN=23*0., 0.117, 126*0.0,
  SPFN=23*0.0, 0.217, 126*0.0,
  HHTFN=23*0.0, 0.030, 126*0.0, KMET=23*0.0, 12.0, 126*0.0,
  A=.0750, .0630, .0540, .0450, .0300, .0175, .0126, .0126, .0085, .0085,
    .0100, .0100, .0110, .0175, .0225, .0275, .0300, .0300, .0300, .0300,
    .0300, .0260, .0200, .0200, 126*0.0,
  AV=17*0.0, 5*0.042, 128*0.0,
  DH=.2310, .1590, .1560, .1530, .1020, .0820, .0775, .0775, .0696,
    .0696, .0727, .0727, .0746, .0824, .0857, .0880, .0960, .0888,
    .0888, .0828, .0811, .0638, .0980, .0833, 126*0.0,
  DHV=17*0.0, 5*0.136, 128*0.0,
  F=17*0.0, 5*0.09, 128*0.0,  TW=150*1400.,
TIP CAP AND BYPASS FLOW PARAMETERS ——— NTCF=10, NBPI=2, NBPO=18,
  DLBP=0.65, DHBP=0.075, FFBP=0.10, AINBP=.001, PBPRI=0.50,
  RINBP=3.80, AOUTBP=.001, ROUTBP=3.75, ALBPO=36.0,
  IOPHTT=1, NHI=2, DHI=.030,  NHO=3, DHO=.020, PBP=200.0,
  RIH=6.60, RIPL=6.75, SPIH=0.20, ALIMP=90.0,
  DIC=.075, AIMP=.0589, TNIMP=1500. &END
```

Figure 8.—Example 1 input data.

(A(NI − 1) = A(NI)) and the user specifies zero friction and zero heat transfer (no heat addition), the solution may not converge. Without friction or heat addition in the last interval (both of which drive the flow toward choking) the flow will also want to choke at node NI − 1, but this cannot be accommodated. The problem can be circumvented by specifying the exit free flow area A(NI) to be slightly smaller than A(NI − 1).

A complete data input set (for example 1 in the section Example Problems) is shown in figure 8. This input describes the upper flow path of figure 1 and illustrates the use of both tip-cap and bypass flow. Details concerning the preparation of this data input set are given in the section Example Problems.

Program Output

The program output is described in figure 9, which shows the output for example 1. The title is shown first, followed by statements concerning the chosen options for physical properties, coolant flow calculation, rotational speed, whether tip-cap or bypass flow was specified, and if so, in which input intervals. The next statement tells the user whether the output is for the original input frame of reference or for the revised frame of reference (generated from the slices). This statement is followed by a table that shows the specified nodes, the number of slices in each interval, and the slice number (new node number) corresponding to each original input node. This table is important, since all error messages refer to the slice frame of reference. Any problem leading to warning or abort messages in the new frame of reference can be traced back to the input frame of reference with this table.

The next output is a listing of all input data curves, followed by any warning or abort messages and a statement quantifying the overall number of iterations needed to achieve flow convergence.

A tabulation of mostly geometric parameters is next printed out for the following node or interval items:

I	node or interval number
IOPTFI	input option for fake interval specification
IOPTHT	input option for heat transfer specification
IOPTFF	input option for friction factor specification
IOPTCR	input option for heat transfer rotation correction specification
Z	specified or calculated (for NSLI > 1) node z value
R	specified or calculated (for NSLI > 1) node r value
Y	specified or calculated (for NSLI > 1) node y value
A	specified or calculated (for NSLI > 1) node free flow area
DH	specified or calculated (for NSLI > 1) node hydraulic diameter
TW	specified interval wall temperature
DX	calculated straight-line interval distance between nodes (for all fake intervals DX is set to 0.0)
XTOT	flow path length up to that node (summation of DX)
KT	specified total pressure loss coefficient KTSGMT for regular intervals if IOPTFF(I) = 4; or calculated total pressure loss coefficient for fake intervals if IOPTFI(I) = 1; if a friction factor is specified or calculated, KT is shown as zero.
NSLI	number of specified slices in an interval if output is in original input frame of reference; set equal to 1 if output is in new, slice frame of reference.

```
    EXAMPLE PROBLEM 1 (FIGURE 1 UPPER FLOW PATH)


 ENGLISH UNITS

 PHYSICAL PROPERTIES (G, CP, MU AND K) OBTAINED FROM SUBROUTINE AIRPRP

 COOLANT FLOW RATE DETERMINED FROM SPECIFIED INLET AND EXIT PRESSURES

 ROTATIONAL SPEED IS  0.370E+05  RPM

 BYPASS CHANNEL SPECIFIED BETWEEN INTERVALS  2 AND 18

 TIP CAP FLOW SPECIFIED IN INTERVAL 10

 OUTPUT IN ORIGINAL NODE/INTERVAL FRAME OF REFERENCE
 -------------------------
 INPUT  SLICES  SLICE
  NODE     IN     NO.
  NO.  INTERVAL
    1        2      2
    2        1      3
    3        2      5
    4        2      7
    5        1      8
    6        2     10
    7        2     12
    8        2     14
    9        1     15
   10        1     16
   11        1     17
   12        2     19
   13        2     21
   14        2     23
   15        2     25
   16        2     27
   17        1     28
   18        1     29
   19        2     31
   20        2     33
   21        2     35
   22        2     37
   23        1     38
   24        2     40



     CARTESIAN X-AXIS
     CARTESIAN Y-AXIS
 THE INPUT FANNING FRICTION FACTOR CURVE FOR PLAIN PASSAGES IS
         RE4          FFF4
      0.1000E+03  0.1700E+00
      0.5000E+03  0.5400E-01
      0.1000E+04  0.1700E-01
      0.2000E+04  0.8500E-02
      0.2500E+04  0.7000E-02
      0.3000E+04  0.7700E-02
      0.3500E+04  0.1000E-01
      0.4000E+04  0.1070E-01
      0.5000E+04  0.1000E-01
      0.1000E+05  0.8000E-02
      0.1000E+06  0.4500E-02
      0.1000E+07  0.2900E-02
 -------------------------
     LOGARITHMIC X-AXIS
     LOGARITHMIC Y-AXIS
 THE INPUT COLBURN J-FACTOR CURVE IS
         REJCF          CJF
      0.1000E+03  0.4400E-01
      0.1000E+04  0.4500E-02
      0.2000E+04  0.2300E-02
      0.3000E+04  0.2600E-02
      0.6000E+04  0.3200E-02
      0.1000E+05  0.2900E-02
      0.1000E+06  0.1900E-02
      0.1000E+07  0.1300E-02

     WARNING - IMPINGEMENT FLOW HAS NOT CONVERGED IN SUBROUTINE TIPIMP IN OVERALL FLOW ITERATION  8

     WARNING - IMPINGEMENT FLOW HAS NOT CONVERGED IN SUBROUTINE TIPIMP IN OVERALL FLOW ITERATION  9

 ------------------------------------------------
 CONVERGENCE ACHIEVED IN  27 OVERALL ITERATIONS
 ------------------------------------------------
```

I	OPTIONS (IOPT) FI	HT	FF	CR	Z (IN)	R (IN)	Y (IN)	A (IN**2)	DH (IN)	TW (F)	DX (IN)	XTOT (IN)	KT	NSLI
					0.0000E+00	0.3850E+01	0.0000E+00	0.6250E-01	0.2310E+00				0.5000E+00	
1	0	4	2	0	0.4000E+00	0.3850E+01	0.0000E+00	0.7500E-01	0.2310E+00	0.1400E+04	0.4000E+00	0.4000E+00	0.0000E+00	2
2	0	4	2	0	0.5000E+00	0.4000E+01	0.0000E+00	0.6300E-01	0.1590E+00	0.1400E+04	0.1803E+00	0.5803E+00	0.0000E+00	1
3	0	4	2	0	0.4400E+00	0.4350E+01	0.0000E+00	0.5400E-01	0.1560E+00	0.1400E+04	0.3551E+00	0.9354E+00	0.0000E+00	2
4	0	4	2	0	0.3500E+00	0.4650E+01	0.0000E+00	0.4500E-01	0.1530E+00	0.1400E+04	0.3132E+00	0.1249E+01	0.0000E+00	2
5	1	7	7	0	0.3500E+00	0.4650E+01	0.0000E+00	0.3000E-01	0.1020E+00	0.1400E+04	0.0000E+00	0.1249E+01	0.1037E+00	1
6	0	1	1	0	0.2300E+00	0.5350E+01	0.0000E+00	0.1750E-01	0.8200E-01	0.1400E+04	0.7102E+00	0.1959E+01	0.0000E+00	2
7	0	1	1	0	0.2000E+00	0.6020E+01	0.0000E+00	0.1260E-01	0.7750E-01	0.1400E+04	0.6707E+00	0.2629E+01	0.0000E+00	2
8	0	1	1	0	0.2000E+00	0.6430E+01	0.0000E+00	0.1260E-01	0.7750E-01	0.1400E+04	0.4100E+00	0.3039E+01	0.0000E+00	2
9	0	4	4	0	0.2200E+00	0.6430E+01	0.0000E+00	0.8500E-02	0.6960E-01	0.1400E+04	0.2000E-01	0.3059E+01	0.1650E+01	1
10	0	5	4	0	0.4800E+00	0.6430E+01	0.0000E+00	0.8500E-02	0.6960E-01	0.1400E+04	0.2600E+00	0.3319E+01	0.1650E+01	1
11	0	4	4	0	0.5000E+00	0.6430E+01	0.0000E+00	0.1000E-01	0.7270E-01	0.1400E+04	0.2000E-01	0.3339E+01	0.1650E+01	1
12	0	1	1	0	0.5000E+00	0.6100E+01	0.0000E+00	0.1000E-01	0.7270E-01	0.1400E+04	0.3300E+00	0.3669E+01	0.0000E+00	2
13	0	1	1	0	0.5200E+00	0.5550E+01	0.0000E+00	0.1100E-01	0.7460E-01	0.1400E+04	0.5504E+00	0.4220E+01	0.0000E+00	2
14	0	1	1	0	0.7200E+00	0.4950E+01	0.0000E+00	0.1750E-01	0.8240E-01	0.1400E+04	0.6325E+00	0.4852E+01	0.0000E+00	2
15	0	1	1	0	0.9500E+00	0.4550E+01	0.0000E+00	0.2250E-01	0.8570E-01	0.1400E+04	0.4614E+00	0.5314E+01	0.0000E+00	2
16	0	1	1	0	0.1400E+01	0.4000E+01	0.7000E-01	0.2750E-01	0.8800E-01	0.1400E+04	0.7141E+00	0.6028E+01	0.0000E+00	2
17	1	7	7	0	0.1400E+01	0.4000E+01	0.7000E-01	0.3000E-01	0.9600E-01	0.1400E+04	0.0000E+00	0.6028E+01	0.6944E-02	1
18	0	2	0	0	0.1630E+01	0.3850E+01	0.1000E+00	0.3000E-01	0.8880E-01	0.1400E+04	0.2762E+00	0.6304E+01	0.0000E+00	1
19	0	2	0	0	0.1920E+01	0.3600E+01	0.1800E+00	0.3000E-01	0.8880E-01	0.1400E+04	0.3912E+00	0.6695E+01	0.0000E+00	2
20	0	2	0	0	0.2550E+01	0.3250E+01	0.4700E+00	0.3000E-01	0.8280E-01	0.1400E+04	0.7769E+00	0.7472E+01	0.0000E+00	2
21	0	2	0	0	0.3400E+01	0.3060E+01	0.1150E+01	0.3000E-01	0.8110E-01	0.1400E+04	0.1105E+01	0.8577E+01	0.0000E+00	2
22	0	2	0	0	0.4300E+01	0.3030E+01	0.2350E+01	0.2600E-01	0.6380E-01	0.1400E+04	0.1500E+01	0.1008E+02	0.0000E+00	2
23	1	7	7	0	0.4300E+01	0.3030E+01	0.2350E+01	0.2000E-01	0.9800E-01	0.1400E+04	0.0000E+00	0.1008E+02	0.4230E-01	1
24	0	3	5	0	0.4620E+01	0.3030E+01	0.2800E+01	0.2000E-01	0.8330E-01	0.1400E+04	0.5522E+00	0.1063E+02	0.0000E+00	2

Figure 9.—Example 1 program output.

```
TIP CAP FLOW CALCULATIONS IN INTERVAL OR SLICE 10  (  3 ITERATIONS)

   FLOW RATE=     0.18602E-02 (LBM/S)

   NO. OF INLET HOLES  =     2
   INLET HOLE DIAMETER =     0.30000E-01 (IN)
   ALIMP               =     0.90000E+02 (DEG)
   INLET MACH NUMBER   =     0.31109E+00
   INLET DISCH. COEFF. =     0.84388E+00

   CHAMB. TOT. PRESS. (3)=     0.22927E+03 (PSIA)
   CHAMB. MACH NUMBR. (3)=     0.19202E-01
   CHAMB. TOT. PRESS. (4)=     0.23737E+03 (PSIA)
   CHAMB. TOT. TEMP.  (4)=     0.13385E+04 (F)
   IMPINGEMENT H      (4)=     0.14289E+04 (BTU/FT**2/HR/R)

   NO. OF OUTLET HOLES =     3
   OUTLET HOLE DIAMETER=     0.20000E-01 (IN)
   OUTLET MACH NUMBER  =     0.51112E+00
   OUTLET DISCH. COEFF.=     0.89111E+00
   OUTLET BACK PRESS.  =     0.20000E+03 (PSIA)
```

I	T (F)	TT (F)	P (PSIA)	PT (PSIA)	W (LBM/S)	V (FT/S)	M	GAMMA	CP BTU/(LBM-R)	VISC. LBM/(FT-S)	TH. CNDT. BTU/(FT-HR-R)
	0.7497E+03	0.7500E+03	0.1748E+03	0.1749E+03	0.9745E-02	0.5757E+02	0.3416E-01	0.137E+01	0.254E+00	0.217E-04	0.285E-01
1	0.7700E+03	0.7701E+03	0.1748E+03	0.1749E+03	0.9745E-02	0.4877E+02	0.2871E-01	0.137E+01	0.255E+00	0.220E-04	0.289E-01
2	0.7765E+03	0.7766E+03	0.1800E+03	0.1801E+03	0.8140E-02	0.4735E+02	0.2780E-01	0.137E+01	0.255E+00	0.220E-04	0.291E-01
3	0.8059E+03	0.8061E+03	0.1932E+03	0.1933E+03	0.8140E-02	0.5269E+02	0.3060E-01	0.136E+01	0.256E+00	0.224E-04	0.296E-01
4	0.8302E+03	0.8305E+03	0.2060E+03	0.2061E+03	0.8140E-02	0.6045E+02	0.3479E-01	0.136E+01	0.257E+00	0.227E-04	0.301E-01
5	0.8298E+03	0.8305E+03	0.2057E+03	0.2061E+03	0.8140E-02	0.9077E+02	0.5224E-01	0.136E+01	0.257E+00	0.227E-04	0.301E-01
6	0.1078E+04	0.1080E+04	0.2310E+03	0.2322E+03	0.8140E-02	0.1652E+03	0.8753E-01	0.135E+01	0.264E+00	0.254E-04	0.348E-01
7	0.1212E+04	0.1216E+04	0.2471E+03	0.2494E+03	0.8140E-02	0.2333E+03	0.1188E+00	0.134E+01	0.268E+00	0.268E-04	0.373E-01
8	0.1264E+04	0.1268E+04	0.2549E+03	0.2572E+03	0.8140E-02	0.2331E+03	0.1171E+00	0.134E+01	0.269E+00	0.273E-04	0.382E-01
9	0.1259E+04	0.1268E+04	0.2459E+03	0.2512E+03	0.8140E-02	0.3572E+03	0.1796E+00	0.134E+01	0.269E+00	0.272E-04	0.381E-01
10	0.1263E+04	0.1269E+04	0.2432E+03	0.2464E+03	0.6280E-02	0.2793E+03	0.1403E+00	0.134E+01	0.269E+00	0.273E-04	0.382E-01
11	0.1265E+04	0.1270E+04	0.2396E+03	0.2418E+03	0.6280E-02	0.2414E+03	0.1212E+00	0.134E+01	0.269E+00	0.273E-04	0.382E-01
12	0.1296E+04	0.1302E+04	0.2084E+03	0.2112E+03	0.6280E-02	0.2823E+03	0.1405E+00	0.134E+01	0.270E+00	0.276E-04	0.387E-01
13	0.1331E+04	0.1339E+04	0.1610E+03	0.1641E+03	0.6280E-02	0.3387E+03	0.1671E+00	0.134E+01	0.271E+00	0.279E-04	0.394E-01
14	0.1360E+04	0.1365E+04	0.1258E+03	0.1274E+03	0.6280E-02	0.2768E+03	0.1355E+00	0.134E+01	0.272E+00	0.282E-04	0.399E-01
15	0.1372E+04	0.1377E+04	0.1101E+03	0.1112E+03	0.6280E-02	0.2678E+03	0.1209E+00	0.134E+01	0.273E+00	0.283E-04	0.401E-01
16	0.1383E+04	0.1388E+04	0.9268E+02	0.9355E+02	0.6280E-02	0.2423E+03	0.1179E+00	0.134E+01	0.273E+00	0.284E-04	0.403E-01
17	0.1384E+04	0.1388E+04	0.9282E+02	0.9354E+02	0.6280E-02	0.2219E+03	0.1079E+00	0.134E+01	0.273E+00	0.284E-04	0.403E-01
18	0.1257E+04	0.1262E+04	0.9076E+02	0.9185E+02	0.7885E-02	0.2653E+03	0.1335E+00	0.134E+01	0.269E+00	0.272E-04	0.381E-01
19	0.1274E+04	0.1280E+04	0.8595E+02	0.8711E+02	0.7885E-02	0.2830E+03	0.1417E+00	0.134E+01	0.270E+00	0.274E-04	0.384E-01
20	0.1302E+04	0.1309E+04	0.7827E+02	0.7957E+02	0.7885E-02	0.3156E+03	0.1569E+00	0.134E+01	0.271E+00	0.276E-04	0.388E-01
21	0.1329E+04	0.1339E+04	0.6971E+02	0.7119E+02	0.7885E-02	0.3599E+03	0.1776E+00	0.134E+01	0.271E+00	0.279E-04	0.393E-01
22	0.1342E+04	0.1365E+04	0.5320E+02	0.5583E+02	0.7885E-02	0.5482E+03	0.2695E+00	0.134E+01	0.272E+00	0.280E-04	0.396E-01
23	0.1325E+04	0.1365E+04	0.5098E+02	0.5564E+02	0.7885E-02	0.7364E+03	0.3638E+00	0.134E+01	0.271E+00	0.279E-04	0.393E-01
24	0.1331E+04	0.1372E+04	0.5000E+02	0.5478E+02	0.7885E-02	0.7533E+03	0.3716E+00	0.134E+01	0.271E+00	0.279E-04	0.394E-01

I	RE	PR	ST	NU	F	FCOR	HC (BTU/FT**2-HR-F)	HCCOR	HCCORC	HTACOR	TAN (F)
1	0.1640E+05	0.6959E+00	0.4178E-02	0.4978E+02	0.7204E-02	0.1000E+01	0.9022E+02	1.0000	1.0000	1.0000	0.7646E+03
2	0.1118E+05	0.6960E+00	0.4366E-02	0.4171E+02	0.7565E-02	0.1000E+01	0.8976E+02	1.0000	1.0000	1.0000	0.7734E+03
3	0.1259E+05	0.6961E+00	0.4473E-02	0.3784E+02	0.7742E-02	0.1000E+01	0.1020E+03	1.0000	1.0000	1.0000	0.7989E+03
4	0.1465E+05	0.6952E+00	0.4347E-02	0.4243E+02	0.7532E-02	0.1000E+01	0.1174E+03	1.0000	1.0000	1.0000	0.8245E+03
5	0.1465E+05	0.6952E+00	0.0000E+00	0.0000E+00	0.0000E+00	0.1000E+01	0.0000E+00	1.0000	1.0000	1.0000	0.0000E+00
6	0.1803E+05	0.6926E+00	0.1607E-01	0.1876E+03	0.3043E+00	0.1000E+01	0.9641E+03	1.0000	1.0000	1.0000	0.1025E+04
7	0.2243E+05	0.6932E+00	0.1507E-01	0.2202E+03	0.3043E+00	0.1000E+01	0.1300E+04	1.0000	1.0000	1.0000	0.1186E+04
8	0.2202E+05	0.6931E+00	0.1486E-01	0.2279E+03	0.3043E+00	0.1000E+01	0.1386E+04	1.0000	1.0000	1.0000	0.1255E+04
9	0.2937E+05	0.6931E+00	0.3853E-02	0.6864E+02	0.1517E+01	0.1000E+01	0.4410E+03	1.0000	1.0000	1.0000	0.1267E+04
10	0.2262E+05	0.6931E+00	0.2898E-02	0.5224E+02	0.1104E+00	0.1000E+01	0.3547E+03	1.0000	1.0000	1.0000	0.1268E+04
11	0.2007E+05	0.6931E+00	0.3998E-02	0.5918E+02	0.1467E+01	0.1000E+01	0.3932E+03	1.0000	1.0000	1.0000	0.1269E+04
12	0.1985E+05	0.6931E+00	0.1532E-01	0.2114E+03	0.3043E+00	0.1000E+01	0.1383E+04	1.0000	1.0000	1.0000	0.1296E+04
13	0.1829E+05	0.6933E+00	0.1560E-01	0.2019E+03	0.3043E+00	0.1000E+01	0.1305E+04	1.0000	1.0000	1.0000	0.1330E+04
14	0.1258E+05	0.6936E+00	0.1706E-01	0.1619E+03	0.3043E+00	0.1000E+01	0.9703E+03	1.0000	1.0000	1.0000	0.1360E+04
15	0.1013E+05	0.6938E+00	0.1832E-01	0.1356E+03	0.3043E+00	0.1000E+01	0.7729E+03	1.0000	1.0000	1.0000	0.1374E+04
16	0.8478E+04	0.6939E+00	0.1934E-01	0.1188E+03	0.3043E+00	0.1000E+01	0.6588E+03	1.0000	1.0000	1.0000	0.1385E+04
17	0.8476E+04	0.6939E+00	0.0000E+00	0.0000E+00	0.0000E+00	0.1000E+01	0.0000E+00	1.0000	1.0000	1.0000	0.0000E+00
18	0.1029E+05	0.6931E+00	0.1168E-01	0.9119E+02	0.9000E-01	0.1000E+01	0.3209E+03	1.0000	1.0000	1.0000	0.1324E+04
19	0.1023E+05	0.6931E+00	0.1170E-01	0.9081E+02	0.9000E-01	0.1000E+01	0.3161E+03	1.0000	1.0000	1.0000	0.1275E+04
20	0.9445E+04	0.6932E+00	0.1174E-01	0.9021E+02	0.9000E-01	0.1000E+01	0.3159E+03	1.0000	1.0000	1.0000	0.1302E+04
21	0.9163E+04	0.6933E+00	0.1177E-01	0.8962E+02	0.9000E-01	0.1000E+01	0.3157E+03	1.0000	1.0000	1.0000	0.1331E+04
22	0.8279E+04	0.6934E+00	0.1179E-01	0.8933E+02	0.9000E-01	0.1000E+01	0.3162E+03	1.0000	1.0000	1.0000	0.1357E+04
23	0.1664E+05	0.6933E+00	0.0000E+00	0.0000E+00	0.0000E+00	0.1000E+01	0.0000E+00	1.0000	1.0000	1.0000	0.0000E+00
24	0.1411E+05	0.6933E+00	0.4553E-02	0.4656E+02	0.6991E-02	0.1000E+01	0.2575E+03	1.0000	1.0000	1.0000	0.1366E+04

```
   BYPASS FLOW BETHEEN INTERVALS OR SLICES  2 AND 18
     (CONVERGED IN  3 ITERATIONS)
       FLOW RATE=     0.16056E-02 LBM/S
       DX        =     0.65000E+00 IN
       DHYD      =     0.75000E-01 IN
       FR. FCT   =     0.10000E+00
   INLT. PR. REC.=     0.50000E+00
```

	A (IN**2)	R (IN)	TT (F)	T (F)	PT (PSIA)	P (PSIA)	M	V (FT/S)	ALPHA (DEG)
IN	0.1000E-02	0.3800E+01	0.7733E+03	0.7413E+03	0.1775E+03	0.1609E+03	0.3809E+00	0.6395E+03	0.9000E+02
OUT	0.1000E-02	0.3750E+01	0.8099E+03	0.7157E+03	0.1223E+03	0.9175E+02	0.6610E+00	0.1098E+04	0.3600E+02

Figure 9.—Concluded.

Note that a value of Z, R, Y, A, DH, and KT is shown before the numbered node or interval values. These are the inlet values of position, area, hydraulic diameter, and KTIN, respectively.

A complete description of the specified tip-cap geometry and the calculated tip-cap flow follows. The output is self-explanatory, but the user should be aware that the tip-cap flow calculations do not account for radius change (pumping) in the impingement or exit holes. This does not introduce any significant errors, since for any realistic design the

impingement and exit hole lengths will be kept as short as possible. The tip-cap flow calculations also have no provisions for calculating reverse flow. If too high a backpressure is specified at the tip cap, the tip-cap flow will not converge. This will be noted by appropriate error messages up to and including the final overall flow iteration. The obtained flow solution, although meaningless for the tip-cap geometry, is the same as the solution that would have been obtained had no tip-cap flow been specified.

The next tabulation presents calculated flow properties and physical properties. As before, the inlet values precede the numbered node values (all values in this table are node values). The tabulated parameters are

I	node number
T	static temperature
TT	total temperature
P	static pressure
PT	total pressure
W	coolant flow rate
V	velocity
M	Mach number
GAMMA	ratio of specific heats
CP	specific heat at constant pressure
VISC.	viscosity
TH. CNDT.	thermal conductivity

Note that for rotating turbomachinery (RPM $\neq$ 0) the shown total temperature and total pressure, as well as velocity and Mach number, represent values in the rotating reference frame.

The next tabulation is a mixture of flow and heat transfer parameters, along with specified correction factors. The tabulated parameters are

I	node or interval number
RE	node Reynolds number based on hydraulic diameter (DH)
PR	node Prandtl number
ST	interval Stanton number based on uncorrected HC
NU	interval Nusselt number based on uncorrected HC
F	specified or calculated interval Fanning friction factor
FCOR	specified interval friction factor correction
HC	specified or calculated interval heat transfer coefficient without any correction factors
HCCOR	specified interval heat transfer coefficient correction factor
HCCORC	calculated interval heat transfer correction factor due to rotation (listed as 1.0 if IOPTCR(n) = 0)
HTACOR	specified interval heat transfer area correction factor
TAW	calculated interval adiabatic wall temperature (listed as 0.0 for fake intervals)

Further explanation is in order for the following calculated interval output parameters: ST, NU, F, HC, HCCORC, and TAW (excluding F and HC if they are user specified). If the slice option is used (NSLI(n) > 1) together with the option for printing output at all the slices (ISLOUT = 1), it is obvious that the shown interval values correspond exactly with the slice interval numbers. However, if the slice option is used together with the option for printing output in the original frame of reference (ISLOUT = 0), an arbitrary decision must be made as to which of the calculated slice interval values (the slice intervals that were obtained from the original input interval) will be printed. For the described combination of options (NSLI(n) > 1 and ISLOUT = 0), the shown calculated interval values (ST, NU, F, HC, HCCORC, and TAW) are the values for the last (highest numbered) slice interval in the original input interval.

The final output is a tabulation of bypass flow parameters including a listing of values at the bypass inlet and exit. This output is self-explanatory, except for the following item: CPF has no provision for calculating reverse flow in the bypass channel. If the main coolant flow cannot be balanced without reverse flow in the bypass, the bypass flow is set to zero and the main coolant flow calculations are carried through to convergence. The bypass flow output will show zero flow, as well as zero velocity and Mach number. The obtained solution, although meaningless for the specified bypass geometry, is the same as the solution that would have been obtained had no bypass been specified. The user is therefore cautioned to always check that the calculated bypass flow rate is greater than zero.

Error Messages

All DO loops in CPF have appropriate error messages that are printed if convergence is not achieved. A detailed listing of the error messages will not be provided here, since most messages are self-explanatory and contain a suggested course of action to alleviate the problem. The following comments, however, should be helpful in understanding the error messages:

(1) All error messages stating node or interval numbers refer to the calculated slice frame of reference.

(2) Error messages pertaining to bypass or tip-cap flow are often caused by specifying too large a flow area.

(3) Error messages fall into two general groups: warning messages and abort messages. Program execution continues after a warning message is issued and terminates after an abort message.

(4) Although not all warning messages use the word "WARNING," all messages that result in program termination use the word "ABORT."

(5) Most warning messages have the following generalized format:

WARNING—XXXXX HAS NOT CONVERGED IN OVERALL FLOW ITERATION XX

These messages can be triggered by extreme initial conditions during the iteration process. The solution is valid if the warning messages are for an overall flow iteration number XX that is less than the required number of total overall iterations NTOT. This number (NTOT) is shown following the listing of any warning messages in the following statement:

CONVERGENCE ACHIEVED IN NTOT
OVERALL ITERATIONS

(6) The user is cautioned that it is possible to specify configurations or situations that have no physical solution. These are usually caused by specifying the flow option IOPTW = 1 while also specifying incompatible inlet and exit flow areas and pressures, as well as possibly unrealistic friction factors or heat transfer coefficients. For such cases the following error message is printed out:

ABORT—COOLANT FLOW HAS NOT CONVERGED
IN 100 ITERATIONS

For this error message a suggested course of action is described under Miscellaneous Comments in the section Program Input.

Example Problems

The example problems shown in this section were run on an IBM-compatible Amdahl-5869 computer and with an initial version of CPF which had no provision for direct heat addition (see example 3).

Example 1

Example 1 illustrates most of the features of CPF by analyzing the upper flow path of the conceptual cooled radial turbine of figure 1. This figure does not represent a specific cooled radial turbine design but illustrates the various features that CPF can accommodate.

The nodal breakdown of the upper flow path (consisting of 24 nodes) is shown in figure 2, and the detailed data input is shown in figure 8. The plain passage (from the inlet to the start of the turbulators) is modeled by intervals 1 to 4. Specified options for these intervals are IOPTHT = 4 (internal plain-passage correlation) and IOPTFF = 2 (user-input friction factor curve using NPFF4, etc.). Note that interval 2 contains the inlet for the bypass flow (NBPI = 2). Interval 5 is a fake interval that accounts for the sudden area change between the plain passage and the trip-strip passage. Dummy values (equal to 7) are used for IOPTHT and IOPTFF. Intervals 6 to 8 model the trip-strip passage up to the first turn at the tip cap (IOPTHT = 1 and IOPTFF = 1). Interval 9 models the 90° turn via a plain-passage heat transfer correlation (IOPTHT = 4) and a specified K factor (KTSGMT) for friction (IOPTFF = 4). In interval 10 the heat transfer is specified from an input Colburn J-factor curve (IOPTHT = 5 and using NPCJF, etc.), along with a specified K factor for friction (IOPTFF = 4). Interval 10 also feeds the tip-cap flow (NTCF = 10). Interval 11 models the second 90° turn at the tip in the same manner as interval 9 (IOPTHT = 4 and IOPTFF = 4). Intervals 12 to 16 model the trip-strip intervals leading up to the start of the pin fins (IOPTHT = 1 and IOPTFF = 1). Interval 17 is a fake interval that models the sudden area change between the turbulators and the pin fins. As before, a dummy value of 7 is specified for IOPTHT and IOPTFF. Intervals 18 to 22 model the pin-fin passage up to the finned exit (IOPTHT = 2 for heat transfer, along with a user-specified friction factor, IOPTFF = 0). Note that the bypass flow reenters at interval 18 (NBPO = 18). Interval 23 is a fake interval to account for the sudden area change at the finned passage (a dummy value of 7 for IOPTHT and IOPTFF). Interval 24 models the finned exit passage (using IOPTHT = 3 and IOPTFF = 3).

The following discussion, as well as the notes on the left margin of figure 8 further describe and clarify the input. The first line is the title and the second line starts the NAMELIST data set called DATT. The first three lines set overall parameters as well as inlet and exit conditions. Note that English units are specified and that two slices are specified for each of the 24 intervals (NSLI = 24*2). The next four lines specify parameters for the input Fanning friction factor curve, and the following three lines specify the Colburn J-factor input curve. The geometric flow path (at the passage centroid) is described via the parameters Z, R, and Y. There are 24 specified values for each, followed by 126 zeros. These trailing zeros are arbitrary values that further fill the arrays and have no bearing on the calculations. Such fill-in values are used throughout the data input set. The next four lines are the specifications of the options for fake intervals, heat transfer, and friction factor. Note that, where dummy values are needed, the value of 7 is used. The next two lines contain geometric parameters (EDD and PDE) needed for the specified trip-strip heat transfer correlation (IOPTHT = 1), the roughness parameter (DOE) for the specified friction factor correlation (IOPTFF = 3), and specified total pressure loss coefficients (KTSGMT). Note that although these values are needed only for specific intervals, values are assigned for the total array. The next four lines contain parameters needed for the specified finned passage and are followed by eight lines with required area and hydraulic diameter values. Note that the parameters AV and DHV are needed only for the pin-fin passages. The next line contains values of user-specified friction factors (F) and wall temperatures (TW), and the last six lines specify the needed parameters for tip-cap and bypass flow.

The CPF output corresponding to the figure 8 data input is shown in figure 9. The output is in the original node/interval input frame of reference. Note that warning messages appear for overall flow iterations 8 and 9. The warnings can be ignored, since convergence was achieved in 27 overall iterations. Also note that for fake intervals the output values of Stanton number (ST), Nusselt number (NU), friction factor (F), heat transfer coefficient (HC), and adiabatic wall

temperature (TAW) are all shown as zero. Finally, note that, although each interval was specified to be divided into two slices (NSLI = 24*2 in fig. 8), figure 9 shows that for the appropriate intervals (2, 5, 9, 10, 11, 17, 18, and 23) no interval division was allowed (NSLI forced to be 1 for fake intervals, bypass intervals, tip-cap intervals, and intervals with specified KTSGMT).

Example 2

As stated in the section Flow Path Modeling, the free flow area change between nodes or slices defining a "regular" interval determines the accuracy of the flow calculations. Example 2 illustrates the amount of computational error to be expected from various area variations. Two flow paths are analyzed: the first decreasing in area from 10 cm^2 to 5 cm^2, the second increasing in area from 5 cm^2 to 10 cm^2. Both flow paths are modeled with just one interval, which is successively divided into various slice numbers (from 2 to 150). The analysis assumes no friction and no heat transfer (isentropic flow) in order to isolate the effect of area change. Physical properties are assumed to be constant. The input data are shown in figure 10. Note that hydraulic diameter (DH) is set to a dummy value (1.0), since no friction or heat transfer is specified. Inlet total pressure and total temperature are identical for both cases (100 N/cm^2 and 500 K, respectively); exit pressures are 65 and 94 N/cm^2 for the decreasing and increasing area cases, respectively. The fixed weight flows correspond to the specified inlet total and exit static conditions. The calculated results are summarized in table II.

Since no friction or heat transfer is specified, the exit total conditions ideally should be equal to the inlet total conditions. As can be seen, this is not the case, and the changes in total pressure and total temperature from inlet to exit are thus a measure of the flow calculation accuracy. As expected, accuracy increases with an increase in the number of specified

TABLE II.—SUMMARY OF EXAMPLE 2 RESULTS (OUTLET CONDITIONS)

(a) Decreasing flow area

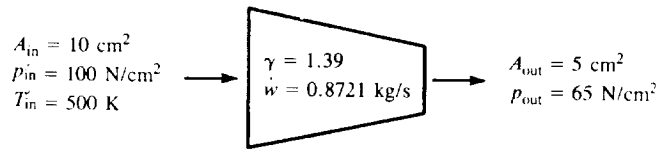

	CPF predictions for number of slices										Insentropic solution
	2	5	10	20	40	60	80	100	125	150	
Temperature, T, K	---	439.1	441.7	442.5	442.7	442.7	442.7	442.7	442.7	442.7	443.1
Total temperature, T', K	---	497.3	498.6	499.0	499.1	499.1	499.1	499.1	499.1	499.1	500.0
Pressure, p, N/cm^2	---	63.69	64.81	65.13	65.23	65.24	65.25	65.25	65.25	65.25	65.0
Total pressure, p', N/cm^2	---	99.27	99.82	99.98	100.0	100.0	100.0	100.0	100.0	100.0	100.0
Mach number, M	---	0.8247	0.8128	0.8094	0.8085	0.8083	0.8083	0.8082	0.8083	0.8083	0.8117

(b) Increasing flow area

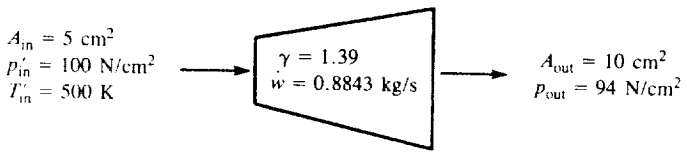

	CPF predictions for number of slices										Insentropic solution
	2	5	10	20	40	60	80	100	125	150	
Temperature, T, K	500.5	495.1	493.3	492.6	492.4	492.3	492.3	492.3	492.3	492.2	491.4
Total temperature, T', K	508.9	503.6	501.9	501.2	501.0	501.0	501.0	500.9	500.9	500.9	500.0
Pressure, p, N/cm^2	97.39	95.12	94.36	94.06	93.96	93.94	93.94	93.93	93.93	93.92	94.0
Total pressure, p', N/cm^2	103.3	101.1	100.4	100.1	99.98	99.96	99.95	99.95	99.94	99.94	100.0
Mach number, M	0.2919	0.2973	0.2991	0.2999	0.3001	0.3001	0.3002	0.3002	0.3002	0.3002	0.2997

```
    EXAMPLE PROBLEM 2 (CALCULATION ACCURACY)
&DATT IECHO=0, IUNITS=1, IOPPRP=0, RG=287.053, RPM=0.0,
G=1.39, CP=0.24, XMU=2.65E-4, XK=0.95E-4,
NI=1,ZIN=0.0, RIN=0.0, YIN=0.0, AIN=10.0, DHIN=1.0,
PTSP=100., TTSP=500., KTIN=0.0, POUT=65.0,
Z=10.0, R=0.0, Y=0.0, A=5.0, IOPTW=0, WIN=0.8721,
IOPTFI=0, IOPTHT=0, IOPTFF=0, NSLI=2,
HC=0.0; DH=1.0, F=0.0, TW=1000. &END
&DATT NSLI=5 &END
&DATT NSLI=10 &END
&DATT NSLI=20 &END
&DATT NSLI=40 &END
&DATT NSLI=60 &END
&DATT NSLI=80 &END
&DATT NSLI=100 &END
&DATT NSLI=125 &END
&DATT NSLI=150 &END
&DATT AIN=5.0, POUT=94.0, A=10.0, WIN=0.8843, NSLI=2 &END
&DATT NSLI=5 &END
&DATT NSLI=10 &END
&DATT NSLI=20 &END
&DATT NSLI=40 &END
&DATT NSLI=60 &END
&DATT NSLI=80 &END
&DATT NSLI=100 &END
&DATT NSLI=125 &END
&DATT NSLI=150 &END
```

Figure 10.—Example 2 input data.

slices. A two-to-one area change from inlet to exit is a severe gradient, and a small number of slices cannot yield an accurate solution. Note that for the decreasing-area case, no solution was obtained for two slices (the calculated exit Mach number exceeded 1.0). Table II shows that, for both cases, solution accuracy increased up to approximately 40 slices but remained essentially unchanged for slice numbers greater than 40.

The fact that the CPF predictions do not match the exact solution is not surprising, since CPF is by nature ill suited for calculating isentropic flow paths (owing to the extensive nested iteration loops in the calculation procedure). The results suggest that sufficient engineering accuracy is obtained if the free flow area change between adjacent nodes or slices is less than 10 percent.

Example 3

Example 3 compares the CPF predictions for both Fanno line and Rayleigh line calculations for Mach numbers between 0.20 and 0.75. Both cases treat a constant-area duct with an inlet area of 10 cm^2 (diameter, 3.568 cm) and an inlet total temperature and pressure of 300 K and 100 N/cm^2, respectively. Weight flow is fixed at 0.7874 kg/s, which results in an inlet Mach number of 0.20. The flow paths are modeled with one interval and various numbers of slices (50, 100, and 150). The input data are shown in figure 11.

A friction factor of 0.10 along with zero heat transfer was chosen to check the Fanno line prediction. From standard Fanno line tables the needed path length to go from Mach 0.20 to 0.75 (with a friction factor of 0.10) is 36.0143 diameters (Z = 36.0143*3.568 = 128.50803 cm in fig. 11). Calculated results are shown in table III for specified slice numbers of 50, 100, and 150. Calculation accuracy increased with slice number, and for 150 slices the predicted results essentially coincided with the Fanno line predictions.

```
    EXAMPLE PROBLEM 3 (FANNO AND RAYLEIGH LINE)
&DATT IECHO=0, IUNITS=1, IOPPRP=0, RG=287.053, RPM=0.0,
G=1.40, CP=0.23978, XMU=1.8E-4, XK=0.6E-4,
NI=1, ZIN=0.0, RIN=0.0, YIN=0.0, AIN=10.0, DHIN=3.56825,
IOPTW=0, WIN=.787355,
PTSP=100.0, TTSP=300.0, KTIN=0.0,
Z=128.50803, R=0.0, Y=0.0, NSLI=50, A=10.0, HC=0.0, DH=3.56825,
F=0.10, TW=500. &END
&DATT NSLI=100 &END
&DATT NSLI=150 &END
&DATT Z=12.576, F=0.0, HC=2.0, TW=2000., NSLI=50 &END
&DATT Z=12.574, NSLI=100 &END
&DATT Z=12.572, NSLI=150 &END
```

Figure 11.—Example 3 input data.

TABLE III.—SUMMARY OF EXAMPLE 3 RESULTS

(a) CPF Fanno line predictions. Friction factor, 0.10; path length, 36.0143 diameters.

	Inlet conditions	Outlet conditions			
		CPF predictions for number of slices			Fanno solution
		50	100	150	
Temperature, T, K	297.6	268.9	269.5	269.6	269.6
Total temperature, T', K	300.0	299.7	299.9	299.9	300.0
Pressure, p, N/cm^2	97.25	24.46	24.66	24.68	24.69
Total pressure, p', N/cm^2	100.0	35.72	35.83	35.84	35.85
Mach number, M	0.20	0.756	0.751	0.750	0.750

(b) CPF Rayleigh line predictions. Arbitrary heat transfer coefficient and wall temperature; path length varied to produce desired exit Mach number.

	Inlet conditions	Outlet conditions			
		CPF predictions for number of slices			Rayleigh solution
		50	100	150	
Temperature, T, K	297.6	1461	1461	1460	1461
Total temperature, T', K	300.0	1625	1625	1625	1625
Pressure, p, N/cm^2	97.25	57.45	57.45	57.45	57.45
Total pressure, p', N/cm^2	100.0	83.43	83.43	83.43	83.44
Mach number, M	0.20	0.750	0.750	0.750	0.750
Path length, cm		12.576	12.574	12.572	-----

Closed-form solution Rayleigh line results are based on fixed levels of heat flux into the fluid. Since the initial version of CPF (by which this example was calculated) did not accommodate specified levels of heat flux directly, comparison of results had to be based on factors other than total heat flux. For the CPF calculations an arbitrary heat transfer coefficient and wall temperature were specified (HC = 2.0 cal/cm^2 s K and TW = 2000.0 K), along with zero friction factor. Path length was varied until the desired exit Mach number (0.75) was reached. The input data are shown in figure 11 (last three lines). A comparison of the calculated exit temperatures and pressures (for the various slice numbers) is shown in table III.

All three cases match the Rayleigh solution temperatures and pressures. Note, however, that slightly different path lengths had to be specified for the various slice numbers. Appendix E describes a feature added to CPF by which the Rayleigh line problem can be solved directly. A heat generation term has been added to the energy equation; an example problem is illustrated for both positive and negative heat generation, and agreement is shown with the closed-form solution.

Concluding Remarks

A computer program called Coolant Passage Flow (CPF) has been developed that calculates the coolant's flow rate, temperature, pressure, and velocity and the heat transfer coefficients inside turbomachinery cooling passages. Flow can be bled off for tip-cap impingement cooling, and a flow bypass can be specified in which coolant flow is taken off at one point in the flow channel and reintroduced at a point farther downstream in the same channel. Although specifically developed for radial turbomachinery, CPF can be used to analyze any turbomachinery coolant geometry that consists of a single flow passage with a single inlet and exit. CPF integrates the one-dimensional momentum and energy equations along a defined passage, taking into account area change, mass addition and subtraction, pumping, friction, and heat transfer. CPF predictions closely agree with closed-form solutions for isentropic flow, Fanno line flow, and Rayleigh line flow. Although the present version of CPF does not allow generalized flow branching, this ability is being developed. Reference 5 is a preliminary report describing an extension of CPF that includes a larger number of available heat transfer and friction factor specification options.

For the flow passage geometries that it is designed to accommodate, CPF will give quick and accurate solutions. It is hoped that turbomachinery designers will find CPF to be a useful tool.

Lewis Research Center
National Aeronautics and Space Administration
Cleveland, Ohio, February 26, 1990

Appendix A
Symbols

A	area, m^2; ft^2
C_D	discharge coefficient; defined as ratio of actual to ideal flow
$C1$, $C2$, CT	constants
C_p	specific heat at constant pressure, cal/(g K); Btu/(lbm °R)
D	diameter, m; ft
D_h	hydraulic diameter, $4A/P$, m; ft
e	surface roughness, m; ft
e^+	parameter defined by $e^+ = \mathrm{Re}(e/D)\sqrt{f/2}$
f	Fanning friction factor, $\Delta p D_h g_c / 2\ell V^2 \rho$
g_c	force-mass conversion constant, 1; 32.174(lbm ft)/(lbf s^2)
h	enthalpy, J/kg; Btu/lbm
h_c	coolant heat transfer coefficient, cal/(m^2 hr K); Btu/(ft^2 hr °R)
J	Colburn J-factor, $h_c(\mathrm{Pr})^{2/3}/\rho V C_p$
K_T	total pressure loss coefficient (K factor), $\Delta p'/(1/2\rho V^2)$
k	thermal conductivity, cal/(m hr K); Btu/(ft^2 hr °R)
L	total length of flow path to a particular node, m; ft
L_f	half-height of a fin (fig. 6), m; ft
ℓ	interval length, m; ft
M	Mach number
m	fin spacing (fig. 6), m; ft
N	rotational speed, 1/s
Nu	Nusselt number, $h_c D_h/k$ = (St)(Re)(Pr)
P	perimeter, m (ft)
Pr	Prandtl number; $C_p\mu/k$
p	pressure, N/m^2; psia (or trip-strip spacing (fig. 5), m; ft)
R	gas constant, J/(kg K); (ft lbf)/(lbm °R)
Ra	Rayleigh number, $rN^2\ (1/T)(T_w - T_{aw})D_h^3 \times \mathrm{Pr}/(\mu/\rho)^2$
Re	Reynolds number, $\rho V D_h/\mu$
Rs	Rossby number, ND_h/V
r	radius, m; ft
S	total heat transfer area of pin-fin interval, m^2; ft^2
St	Stanton number, Nu/(Re)(Pr) = $h_c/\rho V C_p$
T	temperature, K; °R
V	velocity, m/s; ft/s (or open volume in pin-fin interval, m^3; ft^3)
$\dot{w}$	coolant flow rate, kg/s; lbm/s
x	distance along flow path, m; ft
y	distance in plane perpendicular to both r and z (fig. 1), m; ft
z	distance along axis of rotation (fig. 1), m; ft
α	angle between flow path and a perpendicular line to axis of rotation, deg
γ	ratio of specific heats
Λ	recovery factor; equal to $\sqrt{\mathrm{Pr}}$ or $(\mathrm{Pr})^{0.333}$ (eqs. (B29) and (B30))
μ	viscosity, kg/(m s); lbm/(ft s)
ρ	density, kg/m^3; lbm/ft^3
τ_f	fin thickness (fig. 6), m; ft
φ_f	parameter defined by $\varphi_f = \left(2\bar{h}_{c,\mathrm{pp}}/\bar{k}\bar{\tau}_f\right)^{0.50}$ (eq. (B45))

Subscripts:

aw	adiabatic wall
bp	bypass
ch	choke
F	film
imp	impingement
in	inlet
inj	injection
n	node or interval number
pp	plain passage
ref	reference
S	supply
tc	tip cap
v	based on volume
w	wall
x	component in direction of main-stream flow
2	station at tip-cap inlet
3	station in tip-cap chamber
4	station at tip-cap exit

Superscripts:

$(\,)'$	total conditions
$(\bar{\ })$	arithmetic average
i	interval
nd	nodal

Appendix B
Analysis Equations and Flow Solution Procedure

All flow calculations in CPF are based on one-dimensional, compressible fluid flow for a gas obeying the perfect-gas law.

The following notation will be used throughout appendix B to differentiate between values at node points and interval values: symbols representing nodal values will be shown as plain symbols without modifiers; if the symbol refers to a specific node number, the symbol will be subscripted by the node number. For example, A, T, and C_p represent general nodal values of area, temperature, and specific heat ratio, respectively; A_n, T_n, and $C_{p,n}$ designate those parameters for node n. All symbols representing interval values, including those designating the arithmetic average of bounding nodal values, will be shown with a bar (¯) over the symbol (denoting average value over the interval). Values for specific intervals will again be subscripted by the interval number.

Main Program

The main program starts by setting default values and by checking for incompatibilities between the selected friction and heat transfer options. The specifications for tip-cap and bypass flow are also checked. If any irregularities are found, the program terminates with an appropriate error message.

The chosen input units are next converted to working English units, and the maximum allowable (choked) weight flow at the inlet is calculated (to establish an upper bound on allowable weight flow) as follows:

$$T_{ch} = \frac{T'_S}{1 + \frac{\gamma - 1}{2}} \tag{B1}$$

$$V_{ch} = \left(\gamma R g_c T_{ch}\right)^{0.50} \tag{B2}$$

$$p_{ch} = \frac{p'_S}{\left(1 + \frac{\gamma - 1}{2}\right)^{\gamma/(\gamma-1)}} \tag{B3}$$

$$p'_{ch} = \frac{p'_S - K_{T,in} p_{ch} V_{ch}^2}{2 R g_c T_{ch}} \tag{B4}$$

$$\dot{w} = \frac{p_{ch} V_{ch} A_{in}}{R g_c T_{ch}} \tag{B5}$$

If the physical properties are calculated from subroutine AIRPRP, these calculations are iterative, since γ is then a function of temperature.

Overall flow iteration procedure.—From the specified entrance conditions and an assumed or specified inlet flow rate, the flow solution is obtained by marching along the defined flow path from node to node. If the user chooses to subdivide the input flow intervals into slices (NSLI(n) > 1), the program switches from the input nodal frame of reference to a new, calculated, slice frame of reference, in which new node and interval numbers are created in accordance with the total number of slices. All calculations are performed in the new frame of reference. The required node parameters needed at the new slice node locations are obtained by linear interpolation of the appropriate original input nodal values. Input variables that were specified for the original input intervals are retained for the new intervals (which were created by slicing up the original intervals). For all equations presented in this appendix, references to node or interval numbers can refer to either the original input frame of reference or the new, calculated, slice frame of reference, as appropriate.

The pressure and temperature at each node are calculated from the previous node by

$$p_n = p_{n-1} + \left(\frac{dp}{dx}\right)_n dx_n \tag{B6}$$

$$T_n = T_{n-1} + \left(\frac{dT}{dx}\right)_n dx_n \tag{B7}$$

The derivatives $(dp/dx)_n$ and $(dT/dx)_n$ are derived in appendix D and are as follows:

$$\begin{aligned}\left(\frac{dp}{dx}\right)_n = \frac{1}{C2}\Bigg[&\Bigg\{ C1\left[\frac{\bar{\dot{w}}}{\bar{C}_p}\left(\frac{R g_c \bar{T}}{\bar{p}\bar{A}}\right)^2 + \frac{\bar{T}}{\bar{\dot{w}}} \right. \\ &\left. + \frac{\bar{\dot{w}}}{2\bar{C}_p}\left(\frac{R g_c \bar{T}}{\bar{p}\bar{A}}\right)^2 - \left(\frac{C_{p,inj} T_{inj}}{\bar{\dot{w}}\bar{C}_p} + \frac{V_{inj}^2}{2\bar{\dot{w}}\bar{C}_p}\right)\right] \\ &+ \frac{V_{inj,x}}{\bar{A}} - \frac{2(\bar{\dot{w}}/\bar{A}) R g_c \bar{T}}{\bar{p}\bar{A}} \Bigg\} \left(\frac{d\dot{w}}{dx}\right)_n \\ &+ \left\{ \frac{(\bar{\dot{w}}/\bar{A})^2 R g_c \bar{T}}{\bar{p}\bar{A}} - \frac{C1}{\bar{C}_p \bar{A}}\left(\frac{\bar{\dot{w}} R g_c \bar{T}}{\bar{p}\bar{A}}\right)^2 \right\} \left(\frac{dA}{dx}\right)_n \\ &- \frac{4\bar{f} R g_c \bar{T}(\bar{\dot{w}}/\bar{A})^2}{2\bar{p}\bar{D}_h} + \frac{N^2 \bar{r}\bar{p}}{R g_c \bar{T}}\left(\frac{dr}{dx}\right) \\ &- \frac{4\bar{h}_c \bar{A} C1(\bar{T}_w - \bar{T}_{aw})}{\bar{\dot{w}}\bar{C}_p \bar{D}_h}\Bigg]\end{aligned} \tag{B8}$$

$$\left(\frac{dT}{dx}\right)_n = \frac{1}{CT}\left[-\left\{\frac{\bar{\dot{w}}}{\bar{C}_p}\left(\frac{Rg_c\bar{T}}{\bar{p}\bar{A}}\right)^2 + \frac{\bar{T}}{\bar{\dot{w}}} + \frac{\bar{\dot{w}}}{2\bar{C}_p}\left(\frac{Rg_c\bar{T}}{\bar{p}\bar{A}}\right)^2 - \left(\frac{C_{p,\mathrm{inj}}T_{\mathrm{inj}}}{\bar{C}_p\bar{\dot{w}}} + \frac{V_{\mathrm{inj}}^2}{2\bar{\dot{w}}\bar{C}_p}\right)\right\}\left(\frac{d\dot{w}}{dx}\right)_n + \left\{\frac{1}{\bar{C}_p\bar{A}}\left(\frac{\bar{\dot{w}}Rg_c\bar{T}}{\bar{p}\bar{A}}\right)^2\right\}\left(\frac{dA}{dx}\right)_n + \left\{\frac{1}{\bar{p}\bar{C}_p}\left(\frac{\bar{\dot{w}}Rg_c\bar{T}}{\bar{p}\bar{A}}\right)^2\right\}\left(\frac{dp}{dx}\right)_n + \frac{4\bar{h}_c\bar{A}(\bar{T}_w - \bar{T}_{\mathrm{aw}})}{\bar{\dot{w}}\bar{C}_p\bar{D}_h}\right] \tag{B9}$$

where $V_{\mathrm{inj},x}$ is the component of velocity of the injected gas in the main-stream flow direction and

$$\left(\frac{d\dot{w}}{dx}\right)_n = \frac{\dot{w}_n - \dot{w}_{n-1}}{\ell_n} \tag{B10}$$

$$\left(\frac{dA}{dx}\right)_n = \frac{A_n - A_{n-1}}{\ell_n} \tag{B11}$$

$$\left(\frac{dr}{dx}\right)_n = \frac{r_n - r_{n-1}}{\ell_n} \tag{B12}$$

The constants $C1$, $C2$, and CT are defined as follows:

$$C1 = \frac{(\bar{\dot{w}}/\bar{A})^2 Rg_c}{\bar{p}\left[1 + \dfrac{(\bar{\dot{w}}/\bar{A})^2 R^2 g_c^2 \bar{T}}{\bar{p}^2\,\bar{C}_p}\right]} \tag{B13}$$

$$C2 = 1 - \frac{(\bar{\dot{w}}/\bar{A})^2 Rg_c\bar{T}}{\bar{p}^2} + \frac{C1}{\bar{p}\,\bar{C}_p}\left[\frac{(\bar{\dot{w}}/\bar{A})Rg_c\bar{T}}{\bar{p}}\right]^2 \tag{B14}$$

$$CT = 1 + \frac{(\bar{\dot{w}}/\bar{A})^2 R^2 g_c^2 \bar{T}}{\bar{p}^2\bar{C}_p} \tag{B15}$$

Equations (B6) to (B15) contain variables denoting average values over the interval from node $n-1$ to node n. They are designated by a bar ($\bar{}$) over the symbol. The average geometric parameters ($\bar{r}$, $\bar{A}$, and $\bar{D}_h$) are known, but average flow and heat transfer parameters ($\bar{\dot{w}}$, $\bar{p}$, $\bar{T}$, $\bar{h}$, and $\bar{T}_{\mathrm{aw}}$) and average physical properties ($\bar{C}_p$) must be determined in an iterative manner during the solution marching process. The formulation of equations (B6) to (B15) also places a premium on small step size for calculation accuracy. Although the slice option (NSLI(n) > 1) can be used to generate any number of additional slices, each new node and interval generated by the slice option creates additional array requirements for numerous variables. Depending simply on sufficient slices to get the desired calculation accuracy requires very large array sizes for the program variables.

In order to get additional accuracy without needing an exorbitant number of slices, the program further divides each input or slice interval into smaller sections called steps. New, average, geometric variables (position, area, and hydraulic diameter) are calculated by linear interpolation for each step. Pressure and temperature at the next node (node n) are determined from the previous node (node $n-1$) values by the following iterative procedure, consisting of an inner and an outer iteration.

For the first pass through the equations, all average values of pressure $\bar{p}$ and temperature $\bar{T}$ are assumed to be equal to the starting node (node $n-1$) values. The interval is then divided into four steps and the appropriate average step geometric variables are calculated. The solution is marched to node n, where Mach number, pressure, and temperature are determined. Next, the number of steps is doubled, average step geometric variables are recalculated, and the solution is again marched from node $n-1$ to node n. The calculated Mach number at node n is now compared with the previously calculated Mach number. The doubling of step numbers is repeated until the relative difference between successively calculated Mach numbers at node n is less than 5.0×10^{-5} (relative difference is defined as the absolute value of (New value−Old value)/Old value). This iteration procedure is referred to as the "inner iteration." Note that neither physical properties, friction factors, nor heat transfer coefficients are recalculated at each step. They are based on average values in the interval.

Once the Mach number has converged, the calculated pressure and temperature at node n are used to determine new average values of $\bar{p}$ and T between the nodes. The described inner iteration is repeated (for 4, 8, 16, . . ., etc., number of steps) with the new $\bar{p}$ and $\bar{T}$ values. This overall procedure is referred to as the "outer iteration." It is repeated until the relative differences between successively calculated values of $\bar{p}$ and $\bar{T}$ are less than 5.0×10^{-4}.

The described marching procedure is repeated for each interval from the inlet to the exit. If the flow rate was specified (IOPTW = 0) and all node Mach numbers (except at the exit) are less than 1.0, the solution is obtained in one pass. If a Mach number $\geq$ 1.0 is calculated, the program aborts with an appropriate error message. If the program is to determine the flow rate (IOPTW = 1) and a nodal Mach number $\geq$ 1.0 is calculated anywhere except at the exit, the marching procedure is restarted at the inlet with a reduced weight flow.

Once the exit is reached, the calculated pressure at the last node is compared with the specified exit pressure. A new guess of inlet flow rate is then made, and the marching procedure is repeated until the calculated and specified exit pressures converge. For choked flow at the exit the specified back-pressure is decoupled from the solution.

When a converged solution is reached, the working English units are converted back to the specified input units and the output is printed. The input data set is then scanned for the next input case.

Inlet conditions for bypass and tip-cap flows.—At the inlet to the bypass channel (in interval NBPI) the total pressure and temperature are a function of the assumed inlet pressure recovery factor $K_{T,\mathrm{bp}}$ (input variable PBPRI) and the average interval static and total pressures and temperatures as follows:

$$p'_{\mathrm{bp,in}} = p_{\mathrm{NBPI}} + (p'_{\mathrm{NBPI}} - p_{\mathrm{NBPI}})K_{T,\mathrm{bp}} \tag{B16}$$

$$T'_{\mathrm{bp,in}} = T_{\mathrm{NBPI}} + (T'_{\mathrm{NBPI}} - T_{\mathrm{NBPI}})K_{T,\mathrm{bp}} \tag{B17}$$

where

$$p'_{\mathrm{NBPI}} = \frac{p_{\mathrm{NBPI-1}} + p'_{\mathrm{NBPI}}}{2} \tag{B18}$$

$$p_{\mathrm{NBPI}} = \frac{p_{\mathrm{NBPI-1}} + p_{\mathrm{NBPI}}}{2} \tag{B19}$$

$$T'_{\mathrm{NBPI}} = \frac{T'_{\mathrm{NBPI-1}} + T'_{\mathrm{NBPI}}}{2} \tag{B20}$$

$$T_{\mathrm{NBPI}} = \frac{T_{\mathrm{NBPI-1}} + T_{\mathrm{NBPI}}}{2} \tag{B21}$$

If $K_{T,\mathrm{bp}}$ is zero, the bypass inlet total pressure and temperature are equal to the average static values in interval NBPI; if $K_{T,\mathrm{bp}}$ equals 1.0, the bypass inlet total pressure and temperature are equal to the average total conditions in interval NBPI. The bypass inlet pressure recovery factor (default value, 0.0) must assume a value between 0.0 and 1.0. If a value less than 0.0 or greater than 1.0 is input, the variable is reset to 0.0 and 1.0, respectively.

The inlet total temperature and pressure for tip-cap flow in interval NTCF are assumed to be the arithmetic averages of the static conditions in the interval. That is,

$$T'_{tc,\mathrm{in}} = T_{\mathrm{NTCF}} = \frac{T_{\mathrm{NTCF-1}} + T_{\mathrm{NTCF}}}{2} \tag{B22}$$

$$p'_{tc,\mathrm{in}} = p_{\mathrm{NTCF}} = \frac{p_{\mathrm{NTCF-1}} + p_{\mathrm{NTCF}}}{2} \tag{B23}$$

Friction factor and pressure drop calculations.—The friction factor used in CPF is the Fanning friction factor defined by

$$\Delta p = 4f\left(\frac{\ell}{Dh}\right)\frac{V^2}{2g_c}\rho \tag{B24}$$

Only five correlations for specifying friction or pressure drop in an interval are provided in CPF: (1) user-supplied friction factor, (2) trip-strip correlation, (3) friction factor input curves (for pin fins, finned passages, or plain passages), (4) roughened-plain-passage correlation, and (5) K-factor specification. No attempt is made to accommodate the myriad of available correlations, most of which have a narrow range of geometric applicability. The user can readily program specific correlations into CPF. Note that a broad range of correlations is used and discussed in reference 5.

When user supplied, the friction factor is input via the input variable F(NI). When friction factor curves are input in tabular form as a function of Reynolds number for pin fins, finned passages, and plain passages, the corresponding input friction factor variables are FFF2(NPFF2), FFF3(NPFF3), and FFF4(NPFF4), respectively. For this option the required friction factor is determined through interpolation by subroutine SPLFIT, which will be described separately.

For trip strips (roughened tubes) the friction factor is calculated from a correlation of reference 6.

$$f = \frac{2.0}{\left[2.5\ln\left(\frac{D}{2e}\right) - 3.75 + 0.95\left(\frac{p}{e}\right)^{0.53}\right]^2} \tag{B25}$$

This equation is valid for $10 < p/e < 40$ and $e^+ > 35$, where

$$e^+ = \mathrm{Re}\left(\frac{e}{D}\right)\left(\frac{f}{2}\right)^{1/2} \tag{B26}$$

If the friction factor is to be calculated from the plain-passage correlations of reference 7, subroutine WWWFF is used. This subroutine will be described separately.

If a total pressure loss coefficient K_T is specified for an interval (input variable KTSGMT), it is transformed to a Fanning friction factor as follows:

$$f = \frac{\bar{K}_T\bar{D}_h}{4\ell} \tag{B27}$$

Total pressure losses due to sudden expansions and contractions in fake intervals are calculated by subroutine TPLOSS, which will be described separately.

Heat transfer calculations.—Heat addition to and subtraction from the fluid in each interval are driven by the difference between the specified wall temperature and the calculated adiabatic wall temperature, which is defined by

$$T_{aw} = \bar{T} + \bar{\Lambda}(\bar{T}' - T) \tag{B28}$$

The recovery factor Λ is a function of the average Reynolds number in the interval

$$\bar{\Lambda} = (\mathrm{Pr})^{0.50} \quad \text{for } \mathrm{Re} < 2300 \tag{B29}$$

$$\bar{\Lambda} = (\mathrm{Pr})^{0.333} \quad \text{for } \bar{\mathrm{Re}} \geq 2300 \tag{B30}$$

Physical properties in the heat transfer calculations are evaluated at the reference temperature given by

$$\bar{T}_{ref} = 0.5(\bar{T}_w - T) + \bar{T} \quad \text{for } \mathrm{Re} < 2300 \tag{B31}$$

$$\bar{T}_{ref} = 0.5\ T_w + 0.28\ \bar{T} + 0.22\ \bar{T}_{aw} \quad \text{for } \bar{\mathrm{Re}} \geq 2300 \tag{B32}$$

The Nusselt and Stanton numbers are calculated from the specified or calculated heat transfer coefficient as follows:

$$\mathrm{Nu} = \frac{\bar{h}_c \bar{D}_h}{\bar{k}} \tag{B33}$$

$$\bar{\mathrm{St}} = \frac{\bar{\mathrm{Nu}}}{(\bar{\mathrm{Re}})(\bar{\mathrm{Pr}})} \tag{B34}$$

As for the pressure drop correlations, CPF provides only a limited number (six) of heat transfer correlations for the flow path intervals: (1) user-specified heat transfer coefficient, (2) trip-strip correlation, (3) pin-fin correlation, (4) finned-passage correlation, (5) plain-passage correlation, and (6) input Colburn J-factor curve. There are many other heat transfer correlations in the open literature that the user may wish to incorporate into CPF (most for a limited and quite specific range of geometries). Although the existing heat transfer correlations in CPF have a strictly one-dimensional character, actual internal heat transfer in turbomachinery shows strong three-dimensional effects (such as variations in heat transfer between the passage's leading and trailing surfaces). Such variations are accounted for, in a limited sense, by the expanded number of correlations used and discussed in reference 5.

For trip strips (roughened tubes, IOPTHT = 1) a correlation of reference 6 is used.

$$\bar{\mathrm{St}} = \frac{\frac{\bar{f}}{2}}{1 + \left(\frac{\bar{f}}{2}\right)^{0.5}\left[4.5(\bar{e}^{+})^{0.28}(\bar{\mathrm{Pr}})^{0.57} - 0.95\left(\frac{\bar{p}}{e}\right)^{0.53}\right]} \tag{B35}$$

This equation is valid for $10 < p/e < 40$ and $\bar{e}^{+} > 35$, where e^{+} is given by equation (B26). The heat transfer coefficient is then evaluated from

$$\bar{h}_c = \frac{(\mathrm{St})(\bar{\mathrm{Re}})(\bar{\mathrm{Pr}})(\bar{k})}{\bar{D}_h} \tag{B36}$$

For pin fins (IOPTHT = 2) the correlation of Van Fossen (ref. 8) is used with hydraulic diameter and Reynolds number based on open volume.

$$(\bar{\mathrm{Nu}})_v = 0.153(\bar{\mathrm{Re}})_v^{0.685} \tag{B37}$$

$$\bar{h}_c = \frac{(\mathrm{Nu})_v \bar{k}}{\bar{D}_{h,v}} \tag{B38}$$

For plain passages the heat transfer coefficient is evaluated from an internal correlation (IOPTHT = 4) or from an input J-factor curve (IOPTHT = 5). The internal correlation for laminar flow (Re < 2300) is

$$\bar{h}_c = 4.226\ \frac{\bar{k}}{\bar{D}_h}(\bar{\mathrm{Re}})^{0.01}(\mathrm{Pr})^{0.333} \tag{B39}$$

This formulation is not of the usual form found in the open literature. It was determined from a J-factor curve fit of unpublished engine company data for a rectangular duct with a width to height ratio of 3. The internal correlation for turbulent flow ($\bar{\mathrm{Re}} > 7000$) is

$$\bar{h}_c = 0.023\ \frac{\bar{k}}{\bar{D}_h}(\mathrm{Re})^{0.80}(\mathrm{Pr})^{0.333} \tag{B40}$$

and the internal correlation for transition flow ($2300 \leq \bar{\mathrm{Re}} \leq 7000$) is

$$\bar{h}_c = \mathrm{HL2300} + \frac{\mathrm{HT7000} - \mathrm{HL2300}}{1 - e^{-2.951}} \times \left\{1 - \exp\left[\frac{-2.951(\bar{\mathrm{Re}} - 2300)}{7000 - 2300}\right]\right\} \tag{B41}$$

where HL2300 and HT7000 are equations (B39) and (B40) evaluated at $\bar{\mathrm{Re}}$ equal to 2300 and 7000, respectively. Note that the exact formulation of the laminar and transition equations may not be of great importance, since any practical cooling design will usually have turbulent flow.

If the heat transfer coefficient is obtained from an input Colburn J-factor curve (IOPTHT = 5), it is calculated from

$$h_c = \frac{J\rho V C_p}{(\mathrm{Pr})_F^{0.6667}} \tag{B42}$$

where $(\mathrm{Pr})_F$ is the Prandtl number evaluated at the film temperature

$$\bar{T}_F = 0.5(\bar{T} + \bar{T}_w) \tag{B43}$$

For finned passages (IOPTHT = 3) the heat transfer coefficient is evaluated from

$$h_c = \frac{h_{c,\mathrm{pp}}}{\bar{m} + \bar{\tau}_f}\left[\frac{2\tanh(\bar{\varphi}_f \bar{L}_f)}{\bar{\varphi}_f} + \bar{m}\right] \tag{B44}$$

where

$$\bar{\varphi}_f = \left(\frac{2\bar{h}_{c,\mathrm{pp}}}{\bar{k}\bar{\tau}_f}\right)^{0.50} \tag{B45}$$

and $\bar{h}_{c,\mathrm{pp}}$ is the heat transfer coefficient for a plain passage obtained from equation (B39). The formulation of equation (B44) requires a different heat transfer area to get the proper coolant heat pickup (in eqs. (B8) and (B9)). For all heat transfer options other than finned passages (IOPTHT $\neq$ 3), the effective wetted perimeter is

$$P = \frac{4\bar{A}}{\bar{D}_h} \tag{B46}$$

For finned passages (IOPTHT = 3) the wetted perimeter is based on surface length without the fins, or

$$\bar{P} = 2\,(\text{Number of fins across the interval})(\text{Fin spacing}) \tag{B47}$$

Note that this formulation assumes heat soaking into the fluid from two sides, as shown in figure 6.

The correction factors for heat transfer coefficient due to rotation (HCCORC(NI)) are from references 9 and 10. For radial outflow (ref. 9)

$$\mathrm{HCCORC} = \left[\frac{\mathrm{Ra}}{(\mathrm{Re})^2}\right]^{-0.186} (\mathrm{Rs})^{0.333} \tag{B48}$$

and for radial inflow (ref. 10)

$$\mathrm{HCCORC} = 1.72\left[\frac{\mathrm{Ra}}{(\mathrm{Re})^2}\right]^{0.112} (\mathrm{Rs})^{-0.083} \tag{B49}$$

The Rayleigh and Rossby numbers are given by

$$\mathrm{Ra} = \frac{rN^2\left(\frac{1}{\bar{T}}\right)(\bar{T}_w - \bar{T})\,\bar{D}_h^3\,(\mathrm{Pr})}{\left(\frac{\bar{\mu}}{\bar{\rho}}\right)^2} \tag{B50}$$

$$\mathrm{Rs} = \frac{N\bar{D}_h}{\bar{V}} \tag{B51}$$

Note that equations (B48) and (B49) are valid only for purely radial flow and when the fluid is cooling the wall. If the fluid heats the wall ($\bar{T} > \bar{T}_w$), an appropriate warning message is printed out.

Subroutine BYPSFL

Subroutine BYPSFL (bypass flow) uses simplified versions of equations (B8) and (B9) to determine the flow through the bypass channel in one marching step. The simplifications are the deletion of all heat transfer terms and the use of constant physical properties throughout (evaluated at the average static temperature of interval NBPI if IOPPRP = 1). These assumptions require that the bypass channel be kept short and that the change in flow area from inlet to outlet be kept reasonable.

Subroutine TIPIMP

Subroutine TIPIMP (tip impingement) calculates the flow through an impingement tip cap. The associated flow stations are shown in figure 7. Station 2 represents the inlet holes, station 3 the impingement chamber at the exit of the inlet holes, and station 4 the impingement chamber at the entrance of the exit holes. Station 5 represents the exit holes. The chamber area is assumed to be much greater than the inlet or exit hole areas, giving low throughflow velocity, so that

$$p_3 \simeq p_3' \tag{B52}$$

From the given inlet and exit conditions and an assumed chamber pressure p_3, an inflow and an outflow are calculated. The chamber pressure is then adjusted in successive iterations until the inflow and outflows are equal. Centrifugal pumping effects are included from station 3 to station 4 but not through the inlet or exit holes. Heat pickup is calculated only at the impingement surface (station 4). Heat pickup in the inlet and exit holes is neglected.

Tip-cap inlet flow calculations.—The inlet total conditions at station 2 are assumed to be equal to the static conditions in the tip-cap interval, as shown by equations (B22) and (B23). Inflow static pressure p_2 is assumed to equal the chamber total pressure p_3'. This, together with equation (B52),

implies that

$$p_2 = p_3' \simeq p_3 \tag{B53}$$

For a fixed chamber pressure p_3 an initial guess is made for inlet static temperature, and a new temperature is calculated from

$$V_2 = \left\{ \frac{2\gamma R g_c T_2'}{\gamma - 1} \left[1 - \left(\frac{p_2}{p_2'} \right)^{(\gamma-1)/\gamma} \right] \right\}^{0.50} \tag{B54}$$

$$M_2 = \frac{V_2}{\left[\gamma R g_c T_2' \left(\frac{p_2}{p_2'} \right)^{(\gamma-1)/\gamma} \right]^{0.50}} \tag{B55}$$

$$T_2 = \frac{T_2'}{1 + \frac{\gamma - 1}{2} M_2^2} \tag{B56}$$

This new temperature is compared with the previously used value, and the iteration continues until the calculated temperature converges. The total inflow is obtained from

$$\dot{w}_2 = C_D A_2 \frac{p_2}{R g_c T_2} V_2 \tag{B57}$$

The discharge coefficient C_D is obtained from reference 11 and is shown in figure 12.

The effects of rotation on pressure from station 3 to station 4 are calculated by subroutine BYPSFL. The cross-sectional flow area from station 3 to station 4 is taken as the product of the input impingement cavity diameter (DIC in fig. 7) and the calculated length of the tip-cap flow interval (DX(NTCF)). No heat addition or friction is accounted for, since the flow path is short and the radial flow Mach number will be low. Note, however, that temperature pickup due to impingement is calculated as shown in the next section.

Tip-cap heat transfer calculations.—The temperature increase due to impingement in the chamber is calculated by the Chupp and Helms equation for jets impinging into a concave cavity (ref. 12).

$$(\mathrm{Re})_2 = \frac{\dot{w}_2 D_2}{A_2 \mu_2} \tag{B58}$$

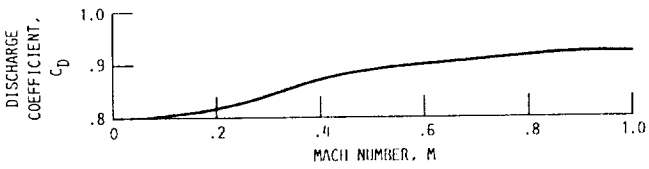

Figure 12.—Tip-cap flow discharge coefficient.

$$h_{\mathrm{imp}} = 0.63 \left(\frac{k}{D_2} \right) (\mathrm{Re})_2^{0.70} \left[\frac{D_2}{(\mathrm{SP})_2} \right]^{0.50} \left(\frac{D_2}{D_4} \right)^{0.60} \times \exp \left[-1.27 \left(\frac{L_{\mathrm{imp}}}{D_4} \right) \left[\frac{D_2}{(\mathrm{SP})_2} \right]^{0.50} \left(\frac{D_2}{D_4} \right)^{1.20} \right] \tag{B59}$$

$$T_4' = T_2' + \frac{h_{\mathrm{imp}} A_2 (T_{w,\mathrm{imp}} - T_2')}{\dot{w}_2 C_p} \tag{B60}$$

where

A_2 total inlet hole area
D_2 inlet hole diameter
$(\mathrm{SP})_2$ inlet hole spacing
L_{imp} impingement distance
D_4 impingement cavity diameter

Tip-cap outlet flow calculations.—Outlet flow is calculated similarly to the inlet flow. Total exit temperature and pressure at station 5 are assumed to be equal to the total conditions at station 4, and the exit static pressure is assumed to be equal to the specified backpressure. With an initial guess for exit static temperature, the calculations proceed as follows:

$$V_5 = \left\{ \frac{2\gamma R g_c T_5'}{\gamma - 1} \left[1 - \left(\frac{p_5}{p_5'} \right)^{(\gamma-1)/\gamma} \right] \right\}^{0.50} \tag{B61}$$

$$M_5 = \frac{V_5}{\left[\gamma R g_c T_5' \left(\frac{p_5}{p_5'} \right)^{(\gamma-1)/\gamma} \right]^{0.50}} \tag{B62}$$

$$T_5 = \frac{T_5'}{1 + \frac{\gamma - 1}{2} M_5^2} \tag{B63}$$

The calculated temperature is compared with the previously used value, and the calculations are repeated until convergence is reached. The exit flow is then calculated from

$$\dot{w}_5 = C_D A_5 \frac{p_5}{R g_c T_5} V_5 \tag{B64}$$

The same discharge coefficient used for the inflow is used for the outflow (fig. 12).

Subroutine TPLOSS

Subroutine TPLOSS (total pressure loss) calculates the total pressure loss due to a sudden expansion or contraction by the

resistance coefficients K_T for pipes (ref. 13). These resistance coefficients (or total pressure loss coefficients) are based on the velocity in the smaller pipe and are defined by

$$K_T \equiv \frac{\Delta p'}{\left(\frac{1}{2}\rho V^2\right)_{\text{smaller pipe}}} \tag{B65}$$

For sudden expansion the total pressure loss coefficient can be expressed analytically as

$$K_T = \left(1 - \frac{A_1}{A_2}\right)^2 \tag{B66}$$

where A_1 is the inlet area and A_2 is the exit area. The curve for sudden contraction was curve fit by the following expressions:

$$X = \left(\frac{A_1}{A_2}\right)^{0.50} \tag{B67}$$

$$K_T = -0.41468\ X^3 + 0.07014\ X^2 - 0.25946\ X + 0.50 \tag{B68}$$

for $0.0 \le X < 0.80$, and

$$K_T = 3.64583\ X^2 - 7.1875\ X + 3.54167 \tag{B69}$$

for $0.80 \le X \le 1.0$; where A_1 is again the inlet area and A_2, the exit area.

Subroutine WWWFF

Subroutine WWWFF (Welty, Wicks, and Wilson friction factors) establishes friction factors for both smooth pipes and rough pipes as shown in reference 7.

Smooth passage.—A passage is considered to be smooth if the specified relative roughness D/e (input parameter DOE) is greater than 1.0×10^6. Reference 7 suggests the following formulas for friction factor:

$$f = \frac{16}{\text{Re}} \quad \text{for Re} < 2300 \text{ (laminar flow)} \tag{B70}$$

$$\frac{1}{\sqrt{f}} = 1.737 \ln\left|(\text{Re})\sqrt{f}\right| - 0.40 \quad \text{for Re} > 3000 \text{ (fully turbulent flow)} \tag{B71}$$

For the Reynolds number range 2300 to 3000 the following equation is assumed:

$$f = \frac{\ln(\text{Re}) - 7.2710}{67.5144} \tag{B72}$$

Equation (B71) is a transcendental equation and is solved by Newton's method.

Roughened passage.—A passage is considered to be rough if the specified relative roughness D/e (input parameter DOE) is less than 1.0×10^6. For this case reference 7 suggests the following formulas for friction factor:

$$f = \frac{16}{\text{Re}} \quad \text{for Re} < 2300 \text{ (laminar flow)} \tag{B73}$$

For fully developed turbulent flow the friction factor expression is not a function of Reynolds number and is given by

$$\frac{1}{\sqrt{f}} = 1.737 \ln\left(\frac{D}{e}\right) + 2.28 \tag{B74}$$

This formula is valid for

$$\frac{\left(\frac{D}{e}\right)}{(\text{Re})\sqrt{f}} < 0.01 \tag{B75}$$

For the transition region the friction factor is a function of both Reynolds number and relative roughness and is given by

$$\frac{1}{\sqrt{f}} = 1.737 \ln\left(\frac{D}{e}\right) + 2.28 - 1.737 \ln\left[4.67 \frac{\left(\frac{D}{e}\right)}{(\text{Re})\sqrt{f}} + 1\right] \tag{B76}$$

The equation is valid for

$$\frac{\left(\frac{D}{e}\right)}{(\text{Re})\sqrt{f}} \ge 0.01 \tag{B77}$$

and is again solved by Newton's method.

Subroutine AIRPRP

Subroutine AIRPRP (air properties) calculates physical properties for unvitiated air from ambient to stoichiometric temperatures. The physical properties are specific heat ratio, specific heat, viscosity, and thermal conductivity. They are evaluated from curve fits of the charts of reference 14. Below 1650 °C (3000 °F) the calculated values are independent of pressure; above that temperature the generated values are valid only for a pressure of 3 atmospheres.

Subroutine SPLFIT

Subroutine SPLFIT (spline fit) generates a spline curve fit from each input set of tabular data. The tabular data set must consist of at least 3 but not more than 25 points. The curve-fitting procedure requires the slopes at the end points. These slopes are calculated from the first two and last two data points. For this reason these points must be chosen such that a straight line between them gives a good approximation to the slope of the curve at the end points. If the calling program calls for a value at an x location outside the range of the input table, the value at the nearest end point is used.

Appendix C
Input Variables

Input parameter[a]	Description and units	Variable type[b]	Default value
	Overall parameters		
TITLE	Title of up to 80 alphanumeric characters	--------	-----
IECHO	Option for input echo: 0—no input echo 1—input echo	I	1
ISLOUT	Option for printing output at slice locations: 0—print only at original input nodes 1—print at all slices		0
IUNITS	Units for input variables: 0—English units 1—SI units		0
IOPPRP	Option for physical properties specification: 0—user specifies G, CP, XMU, and XK 1—properties obtained from subroutine AIRPRP		1
G	Specific heat ratio[c]	R	-----
CP	Specific heat at constant pressure,[c] cal/(g K); Btu/(lbm °R)		-----
XMU	Viscosity,[c] g/(cm s); lbm/(ft s)		-----
XK	Thermal conductivity,[c] cal/(cm s K); Btu/(ft hr °R)		-----
RG	Gas constant, J/(kg K); (ft lbf)/(lbm °R)		-----
RPM	Rotative speed, rpm		-----
NI	Number of intervals in flow passage	I	-----
ZIN	Inlet z location, cm; in.	R	-----
RIN	Inlet r location, cm; in.		-----
YIN	Inlet y location, cm; in.		-----
AIN	Inlet free flow area, cm^2; $in.^2$		-----
DHIN	Inlet hydraulic diameter, cm; in.		-----
IOPTW	Option for coolant flow rate: 0—user specifies coolant flow rate (WIN) 1—program calculates coolant flow rate from specified inlet and exit pressures (PTSP and POUT)	I	-----
WIN	Coolant inlet flow rate,[d] kg/s; lbm/s	R	-----
PTSP	Inlet total supply pressure, N/cm^2; psia		-----
TTSP	Inlet total supply temperature, K; °F		-----
KTIN	Inlet total pressure loss coefficient		0.50
POUT	Outlet pressure,[c] N/cm^2; psia		-----
	Input curves		
NPFF2	Number of points describing Fanning friction factor curve for pin fins ($3 \leq$ NPFF2 ≤ 25)	I	-----
IXFF2	x axis coordinate indicator: 0—Cartesian 1—logarithmic (base 10)	I	0
RE2	Values of Reynolds number at NPFF2 input points in ascending order	R(NPFF2)	-----
IYFF2	y axis coordinate indicator: 0—Cartesian 1—logarithmic (base 10)	I	0
FFF2	Fanning friction factor values at input points	R(NPFF2)	-----
NPFF3	Number of points describing Fanning friction factor curve for finned passage ($3 \leq$ NPFF3 ≤ 25)	I	-----

Input parameter[a]	Description and units	Variable type[b]	Default value
	Input curves (concluded)		
IXFF3	x axis coordinate indicator: 0—Cartesian 1—logarithmic (base 10)	I	0
RE3	Values of Reynolds number at NPFF3 input points in ascending order	R(NPFF3)	-----
IYFF3	y axis coordinate indicator: 0—Cartesian 1—logarithmic (base 10)	I	0
FFF3	Fanning friction factor values at input points	R(NPFF3)	-----
NPFF4	Number of points describing Fanning friction factor curve for plain passage ($3 \leq$ NPFF4 ≤ 25)	I	-----
IXFF4	x axis coordinate indicator: 0—Cartesian 1—logarithmic (base 10)	I	0
RE4	Values of Reynolds number at NPFF4 input points in ascending order	R(NPFF4)	-----
IYFF4	y axis coordinate indicator: 0—Cartesian 1—logarithmic (base 10)	I	0
FFF4	Fanning friction factor values at input points	R(NPFF4)	-----
NPCJF	Number of points describing Colburn J-factor curve ($3 \leq$ NPCJF ≤ 25), $J \equiv h_c(\mathrm{Pr})^{2/3}/\rho VC_p$	I	-----
IXCJF	x axis coordinate indicator: 0—Cartesian 1—logarithmic (base 10)	I	0
RECJF	Values of Reynolds numbers at NPCJF input points in ascending order	R(NPCJF)	-----
IYCJF	y axis coordinate indicator: 0—Cartesian 1—logarithmic	I	0
CJF	Colburn J-factor values at input points	R(NPCJF)	-----
	Nodal and interval parameters		
Z^{nd}	z location, cm; in.	R(NI)	-----
R^{nd}	r location, cm; in.	R(NI)	-----
Y^{nd}	y location, cm; in.	R(NI)	-----
NSLI[i]	Number of slices in each interval	I(NI)	1
IOPTFI[i]	Option for fake interval specification: 0—regular interval 1—fake interval	I(NI)	0
IOPTHT[i]	Option for interval heat transfer calculations: 0—user specifies h via input parameter HC; for this option the user must also specify friction factor via input parameter F 1—trip strips (turbulator correlation of ref. 6); user must input EDD and PDE 2—pin fins (Van Fossen correlation, ref. 8); user must input AV and DHV 3—finned passage; user must input NFNP, THFN, SPFN, HHTFN, and KMET 4—plain passage (internal correlation) 5—user specifies Colburn J-factor curve via input parameters NPCJF, IXCJF, RECJF, IYCJF, and CJF	I(NI)	0

Input parameter[a]	Description and units	Variable type[b]	Default value
Nodal and interval parameters (concluded)			
IOPTFF[f]	Option for Fanning friction factor specification: 0—user specifies f for each interval via input parameter F 1—trip strips (turbulator correlation of ref. 6); friction factors generated from input parameters EDD and PDE 2—obtained from input curves specified by input parameters NPFF2, etc., for pin fins; input parameters NPFF3, etc., for finned passage; input parameters NPFF4, etc., for plain passage 3—obtained from reference 7 correlation for roughened plain passage (must specify DOE) 4—obtained from specified total pressure loss coefficient KTSGMT	I(NI)	0
FCOR[f]	Friction factor correction	R(NI)	1.0
HCCOR[f]	Heat transfer coefficient correction	R(NI)	1.0
HTACOR[f]	Heat transfer area correction	R(NI)	1.0
IOPTCR[f]	Option for calculating rotational heat transfer coefficient correction: 0—no correction 1—correction (specify only for RPM > 0.0)	I(NI)	0
EDD[f]	Relative roughness of trip strips[i]	R(NI)	-----
PDE[f]	Relative rib spacing of trip strips[i]		-----
DOE[f]	Diameter-to-roughness ratio[g] in reference 7 (roughened-passage friction factor correlation)		-----
KTSGMT[f]	Total pressure loss coefficient (may need to correct for path length via HTACOR)		-----
NFNP[f]	Number of finned passages in interval[h]	I(NI)	-----
THFN[f]	Fin thickness,[h] cm; in.	R(NI)	-----
SPFN[f]	Fin center-to-center spacing,[h] cm; in.		-----
HHTFN[f]	Half-height of fin,[h] cm; in.		-----
KMET[f]	Metal thermal conductivity,[h] cal/(cm s K); Btu/(ft hr °R)		-----
A^{nd}	Cross-sectional area based on minimum free flow area, cm^2; $in.^2$		-----
AV[f]	Cross-sectional area based on open volume,[j] V/L, cm^2; $in.^2$		-----
HC[f]	Coolant heat transfer coefficient,[j] cal/(cm^2 s K); Btu/ft^2 hr °R)		0.0
DH^{nd}	Hydraulic diameter based on minimum free flow area ($D_h \equiv 4A/P$), cm; in.		-----
DHV[f]	Hydraulic diameter based on open volume,[j] $4V/S$, cm; in.		-----
F[f]	Fanning friction factor[k]		0.0
TW[f]	Inside wall temperature, K; °F		-----
Q[f]	Heat generation, J/kg; Btu/lbm (see appendix E)		0.0
Parameters specifying locations of tip-cap and bypass flow			
NTCF	Interval from which tip-cap flow is specified	I	-----
NBPI	Interval containing start of bypass channel	I	-----
NBPO	Interval containing exit of bypass channel	I	-----

Input parameter[a]	Description and units	Variable type[b]	Default value
	Tip-cap parameters for interval NTCF		
IOPHTT	Option for tip-cap flow heat transfer calculations: 0—no heat transfer calculations (flow only) 1—heat transfer based on reference 12 (correlation for impinging jets into concave cavity)	I	0
NHI	Number of tip-cap inlet holes	I	-----
DHI	Diameter of tip-cap inlet holes, cm; in.	R	-----
NHO	Number of tip-cap outlet holes	I	-----
DHO	Diameter of tip-cap outlet holes, cm; in.	R	-----
PBP	Tip-cap outlet hole backpressure, N/cm^2; psia		-----
RIH	Radius at inlet holes (must be greater than R(NTCF)), cm; in.		-----
RIPL	Radius at impingement plane (must be greater than RIH), cm; in.		-----
SPIH	Spacing of impingement holes, cm; in.		-----
ALIMP	Angle between main-stream flow and impingement flow,[l] deg		90.0
DIC	Diameter of impingement cavity, cm; in.		-----
AIMP	Impingement cavity heat transfer area, cm^2; $in.^2$		-----
TWIMP	Impingement cavity wall temperature, K; °F		-----
	Bypass channel parameters		
DLBP	Channel length, cm; in.	R	-----
DHBP	Channel hydraulic diameter, cm; in.		-----
FFBP	Channel Fanning friction factor		-----
AINBP	Inlet area, cm^2; $in.^2$		-----
PBPRI	Pressure recovery at inlet ($0.0 \leq PBPRI \leq 1.0$)		0.0
RINBP	Inlet radius, cm; in.		-----
ALBPI	Angle that describes component of exiting flow in main-stream direction in interval NBPI,[l] deg		90.0
AOUTBP	Outlet area, cm^2; $in.^2$		-----
ROUTBP	Outlet radius, cm; in.		-----
ALBPO	Angle that describes component of entering flow in main-stream direction in interval NBPO (fig. 3), deg		90.0

[a]Superscript *i* denotes an interval value; superscript *nd* denotes a nodal value.

[b]I denotes unsubscripted integer value; I( ) denotes subscripted integer value.
R denotes unsubscripted real value; R( ) denotes subscripted real value.

[c]Input only if IOPPRP = 0

[d]Input only if IOPTW = 0

[e]Input only if IOPTW = 1

[f]Input only if IOPTHT = 1

[g]Input only if IOPTFF = 3

[h]Input only if IOPTHT = 3

[i]Input only if IPOTHT = 2

[j]Input only if IOPTHT = 0

[k]Input only if IOPTFF = 0

[l]Dummy variable (not presently used).

Appendix D
Derivation of One-Dimensional Momentum and Energy Equations

Equations (B8) and (B9) are derived in this appendix. They represent formulations of the one-dimensional momentum and energy equations, respectively, which can be integrated along the flow path.

Momentum Equation

Consider the flow of fluid through a control volume in a flow path rotating with speed N about an axis as shown in the sketch. The distance along the flow path is x, and the distance from the rotation axis is r.

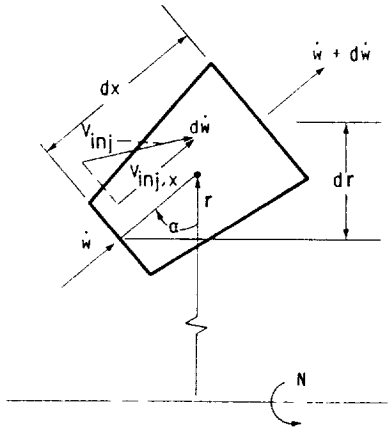

Fluid is injected at a rate $d\dot{w}$ at velocity V_{inj}, having a velocity component in the main-stream flow direction of $V_{inj,x}$. The momentum equation states

$$\text{Change in momentum flow rate (out-in)} = \sum \text{Forces (pressure, friction, and body)}$$

The friction force is expressed by the Fanning friction factor as

$$\frac{1}{2}\rho V^2 f P\, dx \tag{D1}$$

From the definition of hydraulic diameter

$$D_h = \frac{4A}{P} \tag{D2}$$

the friction force becomes

$$\frac{1}{2}\rho V^2 f \frac{4A}{D_h}\, dx \tag{D3}$$

The centrifugal pumping force component acting on the control volume and directed along the flow-path axis is expressed as mass times acceleration by

$$\rho\left(A + \frac{dA}{2}\right) dx\; rN^2 \cos\alpha \tag{D4}$$

where the angle α is as shown in the preceding sketch. Since

$$\cos\alpha = \frac{dr}{dx} \tag{D5}$$

and after neglecting second-order terms (products of differentials), the centrifugal force component becomes

$$rN^2 \rho A\, dr \tag{D6}$$

The forces acting on the control volume are represented in the following sketch:

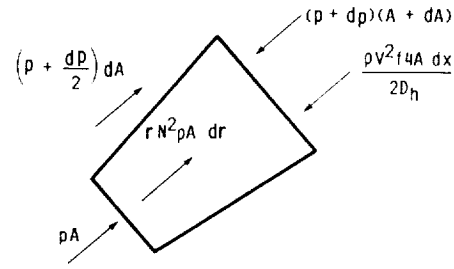

The body force due to the Coriolis acceleration will always act normal to the flow path and makes no contribution along the flow direction. The momentum equation thus becomes

$$(\dot{w} + d\dot{w})(V + dV) - \left[\dot{w}V + V_{inj,x}\, d\dot{w}\right]$$

$$= pA + \left(p + \frac{dp}{2}\right)dA - (p + dp)(A + dA)$$

$$- \frac{\rho V^2 f 4A}{2D_h}\, dx + rN^2 \rho A\, dr \tag{D7}$$

Expanding and dropping second-order terms results in

$$\dot{w}\, dV + V d\dot{w} - V_{inj,x}\, d\dot{w} = -A\, dp - \frac{\rho V^2 f 4A}{2D_h}\, dx$$

$$+ rN^2 \rho A\, dr \tag{D8}$$

Dividing by dx and combining $\dot{w}\,dV$ and $V\,d\dot{w}$ gives

$$\frac{d}{dx}(\dot{w}V) - V_{\text{inj},x}\frac{d\dot{w}}{dx} = -A\frac{dp}{dx} - \frac{\rho V^2 f 4A}{2D_h} + rN^2\rho A\frac{dr}{dx} \tag{D9}$$

The left-most term is expanded by using the perfect-gas law and

$$V = \frac{\dot{w}}{\rho A} \tag{D10}$$

Thus,

$$\dot{w}V = \frac{\dot{w}^2 Rg_c T}{pA} \tag{D11}$$

and

$$\frac{d}{dx}(\dot{w}V) = \frac{2\dot{w}Rg_c T}{pA}\frac{d\dot{w}}{dx} + \dot{w}^2 Rg_c \times\left(\frac{1}{pA}\frac{dT}{dx} - \frac{T}{pA^2}\frac{dA}{dx} - \frac{T}{Ap^2}\frac{dp}{dx}\right) \tag{D12}$$

The momentum equation can then be written as

$$\left(\frac{2\dot{w}Rg_c T}{pA} - V_{\text{inj},x}\right)\frac{d\dot{w}}{dx} + \frac{\dot{w}^2 Rg_c}{pA}\frac{dT}{dx} - \frac{\dot{w}^2 Rg_c T}{pA^2}\frac{dA}{dx} - \frac{\dot{w}^2 Rg_c T}{Ap^2}\frac{dp}{dx} = -A\frac{dp}{dx} - \frac{\rho V^2 f 4A}{2D_h} + rN^2\rho A\frac{dr}{dx} \tag{D13}$$

Solving for dp/dx gives

$$\frac{dp}{dx}\left(A - \frac{\dot{w}^2 Rg_c T}{Ap^2}\right) = \left(\frac{-2\dot{w}Rg_c T}{pA} + V_{\text{inj},x}\right)\frac{d\dot{w}}{dx} - \left(\frac{\dot{w}^2 Rg_c}{pA}\right)\frac{dT}{dx} + \left(\frac{\dot{w}^2 Rg_c T}{pA^2}\right)\frac{dA}{dx} - \frac{\rho V^2 f 4A}{2D_h} + rN^2\rho A\frac{dr}{dx} \tag{D14}$$

Using the perfect-gas law and equation (D10) in the friction and pumping terms and dividing through by A gives the final form of the one-dimensional momentum equation.

$$\frac{dp}{dx} = \frac{\left[\dfrac{-2\left(\frac{\dot{w}}{A}\right)Rg_c T}{pA} + \dfrac{V_{\text{inj},x}}{A}\right]\dfrac{d\dot{w}}{dx} - \dfrac{\left(\frac{\dot{w}}{A}\right)^2 Rg_c}{p}\dfrac{dT}{dx} + \dfrac{\left(\frac{\dot{w}}{A}\right)^2 Rg_c T}{pA}\dfrac{dA}{dx} - \dfrac{4fRg_c T\left(\frac{\dot{w}}{A}\right)^2}{2pD_h} + \dfrac{N^2 rp}{Rg_c T}\dfrac{dr}{dx}}{1 - \dfrac{\left(\frac{\dot{w}}{A}\right)^2 Rg_c T}{p^2}} \tag{D15}$$

Energy Equation

Consider the flow of fluid through the control volume shown in the following sketch:

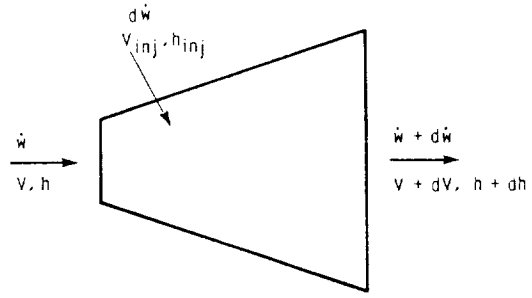

Fluid is injected at a rate $d\dot{w}$ with a velocity V_{inj}. The energy in a gas stream is given by $h + V^2/2$ and the energy equation states that

$$\text{Change in energy flow rate (out-in)} = \sum \text{Heat fluxes by external sources}$$

Assuming that the added heat is due to convection (via the convective heat transfer coefficient h_c), the energy equation can be expressed as

$$(\dot{w} + d\dot{w})\left[h + dh + \frac{(V+dV)^2}{2}\right] - \left(h + \frac{V^2}{2}\right)\dot{w} - \left(h_{\text{inj}} + \frac{V_{\text{inj}}^2}{2}\right)d\dot{w} = h_c P\,dx(T_w - T_{\text{aw}}) \tag{D16}$$

After expanding the left-hand side and neglecting second-order terms, this reduces to

$$\dot{w}\,dh + \dot{w}V\,dV + (h - h_{\text{inj}})d\dot{w} + \left(\frac{V^2}{2} - \frac{V_{\text{inj}}^2}{2}\right)d\dot{w} = h_c P\,dx(T_w - T_{\text{aw}}) \qquad \text{(D17)}$$

Dividing by dx and using

$$h = C_p T \qquad \text{(D18)}$$

$$V = \frac{\dot{w}Rg_c T}{Ap} \qquad \text{(D19)}$$

the energy equation can be arranged to give

$$\dot{w}C_p \frac{dT}{dx} + \frac{\dot{w}Rg_c T}{pA}\frac{d}{dx}\left(\frac{\dot{w}Rg_c T}{pA}\right) + \left[C_p T - C_{p,\text{inj}}T_{\text{inj}} + \frac{1}{2}\left(\frac{\dot{w}Rg_c T}{pA}\right)^2 - \frac{1}{2}V_{\text{inj}}^2\right]\frac{d\dot{w}}{dx} = h_c P(T_w - T_{\text{aw}}) \qquad \text{(D20)}$$

The second term can be expanded to give

$$\frac{d}{dx}\left(\frac{\dot{w}Rg_c T}{pA}\right) = \frac{Rg_c T}{pA}\frac{d\dot{w}}{dx} + \frac{\dot{w}Rg_c}{pA}\frac{dT}{dx} - \frac{\dot{w}Rg_c T}{pA^2}\frac{dA}{dx} - \frac{\dot{w}Rg_c T}{p^2 A}\frac{dp}{dx} \qquad \text{(D21)}$$

Substituting this back into the energy equation and collecting the terms containing dT/dx gives

$$\frac{dT}{dx}\left(\dot{w}C_p + \frac{\dot{w}^2 Rg_c T}{pA}\frac{\dot{w}Rg_c}{pA}\right) = \left[-\frac{\dot{w}^2 Rg_c T}{pA}\frac{Rg_c T}{pA} - C_p T + C_{p,\text{inj}}T_{\text{inj}} - \frac{1}{2}\left(\frac{\dot{w}Rg_c T}{pA}\right)^2 + \frac{1}{2}V_{\text{inj}}^2\right]\frac{d\dot{w}}{dx} + \left[\frac{\dot{w}^2 Rg_c T}{pA}\frac{\dot{w}Rg_c T}{pA^2}\right]\frac{dA}{dx} + \left[\frac{\dot{w}^2 Rg_c T}{pA}\frac{\dot{w}Rg_c T}{p^2 A}\right]\frac{dp}{dx} + h_c P(T_w - T_{\text{aw}}) \qquad \text{(D22)}$$

Dividing through by $\dot{w}C_p$ and using the definition of hydraulic diameter (eq. (D2)) gives the final form of the one-dimensional energy equation.

$$\frac{dT}{dx} = \frac{1}{CT}\left\{-\left[\frac{\dot{w}}{C_p}\left(\frac{Rg_c T}{pA}\right)^2 + \frac{T}{\dot{w}} + \frac{\dot{w}}{2C_p}\left(\frac{Rg_c T}{pA}\right)^2 - \left(\frac{C_{p,\text{inj}}T_{\text{inj}}}{C_p\dot{w}} + \frac{V_{\text{inj}}^2}{2\dot{w}C_p}\right)\right]\frac{d\dot{w}}{dx} + \left[\frac{1}{C_p A}\left(\frac{\dot{w}Rg_c T}{pA}\right)^2\right]\frac{dA}{dx} + \left[\frac{1}{pC_p}\left(\frac{\dot{w}Rg_c T}{pA}\right)^2\right]\frac{dp}{dx} + \frac{4h_c A(T_w - T_{\text{aw}})}{\dot{w}C_p D_h}\right\} \qquad \text{(D23)}$$

where

$$CT = 1 + \frac{\left(\frac{\dot{w}}{A}\right)^2 R^2 g_c^2 T}{p^2 C_p} \qquad \text{(D24)}$$

Marching Equations

Equations (D15) and (D23) are two simultaneous equations in the variables dp/dx and dT/dx. In order to march the solution along the flow path, they must be solved for the individual variables. After substituting the energy equation into the momentum equation (replacing dT/dx) and performing considerable algebraic manipulation, the momentum equation takes the form shown as equation (B8).

$$\frac{dp}{dx} = \frac{1}{C2}\left[\left\{C1\left[\frac{\dot{w}}{C_p}\left(\frac{Rg_c T}{pA}\right)^2 + \frac{T}{\dot{w}} + \frac{\dot{w}}{2C_p}\left(\frac{Rg_c T}{pA}\right)^2 - \left(\frac{C_{p,\text{inj}}T_{\text{inj}}}{C_p\dot{w}} + \frac{V_{\text{inj}}^2}{2\dot{w}C_p}\right)\right] + \frac{V_{\text{inj},x}}{A} - \frac{2\left(\frac{\dot{w}}{A}\right)Rg_c T}{pA}\right\}\frac{d\dot{w}}{dx} + \left\{\frac{\left(\frac{\dot{w}}{A}\right)^2 Rg_c T}{pA} - \frac{C1}{C_p A}\left(\frac{\dot{w}Rg_c T}{pA}\right)^2\right\}\frac{dA}{dx} - \frac{4fRg_c T\left(\frac{\dot{w}}{A}\right)^2}{2pD_h} + \frac{N^2 rp}{Rg_c T}\frac{dr}{dx} - \frac{4h_c AC1(T_w - T_{\text{aw}})}{\dot{w}C_p D_h}\right] \qquad \text{(D25)}$$

where

$$C1 = \frac{\left(\frac{\dot{w}}{A}\right)^2 Rg_c}{p\left[1 + \frac{\left(\frac{\dot{w}}{A}\right)^2 R^2 g_c^2 T}{p^2 C_p}\right]} \qquad \text{(D26)}$$

$$C2 = 1 - \frac{\left(\frac{\dot{w}}{A}\right)^2 Rg_c T}{p^2} + \frac{C1}{pC_p}\left(\frac{\dot{w}Rg_c T}{pA}\right)^2 \qquad \text{(D27)}$$

This value for dp/dx is then substituted into the energy equation (D23) to evaluate dT/dx, and the solution is marched from node to node as explained in appendix B.

Appendix E
Feature of Computer Code for Predicting Coolant Flow and Heat Transfer With Specified Heat Generation

Teresa R. Kline

This appendix describes a feature of the computer code CPF that allows the direct specification of heat generation in a given flow interval. With this feature Rayleigh line flow problems can be solved directly. The appendix provides derivations of the equations, shows input and output, and demonstrates the use and accuracy of the feature via an example problem.

The code originally had no provision for direct heat generation (specifying a desired quantity of energy addition or subtraction in a given flow interval). Heat addition or subtraction was accounted for through a specified or calculated heat transfer coefficient, a heat transfer area, and the temperature difference between the wall and the fluid. This formulation made the quantity of heat addition or subtraction dependent upon the flow path length. The main text demonstrates the accuracy of CPF via example problems for adiabatic flow, Fanno line flow, and Rayleigh line flow. Since Rayleigh line flow involves the direct addition or subtraction of specified quantities of heat (independent of path length), the Rayleigh line flow example problem could not be solved directly. Instead, fixed values of wall temperature and heat transfer coefficient were assumed, and the path length (heat transfer area) was varied until the desired exit Mach number was reached. The calculated exit temperature and pressure were then compared with the closed-form Rayleigh line solution values.

This appendix describes a feature of CPF in which a direct heat generation term (energy per unit mass) added to the energy equation allows the direct solution of the Rayleigh line flow problem. This added feature can also be used to account for heat of vaporization (CPF allows the user to specify gas fluid properties other than those for air). In addition, the revised code can be used to calculate and compare results from heat transfer tests, where known quantities of heat are often added (e.g., via electric heater strips).

This appendix also describes the input and output of the modified code. An illustrative example is given to show the effects of both positive and negative heat generation. The formulation of the energy and marching equations is given with the heat generation term added. CPF is available through the Computer Software Management Information Center (COSMIC), University of Georgia, Athens, Georgia, 30602.

Input

The modified code contains one new input variable, the heat generation per unit mass, Q(I). It is an interval variable and must be specified for each interval. The units are British thermal units per pound mass (Btu/lbm) in the U.S. customary system or joules per kilogram (J/kg) in the International System of Units (SI). The heating term is defaulted as 0.0. If Q = 0.0, we are simply left with the original code. The input value for heat generation is echoed in the output listing, where it is located immediately before the geometric output. Correct units (U.S. or SI) are included.

Derivation of Energy Equation

The momentum equation is the same as that given in the main text, but the energy equation has an added heat generation term. The energy equation is derived as follows:

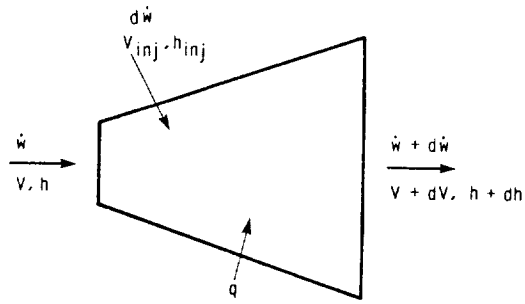

As shown in the sketch, the change in energy flow rate equals the sum of the heat fluxes by external sources:

$$(\dot{w} + d\dot{w})\left\{(h + dh) + \left[\frac{(V + dV)^2}{2}\right]\right\} - \dot{w}\left(h + \frac{V^2}{2}\right) - d\dot{w}\left(h_{inj} + \frac{V_{inj}^2}{2}\right) = h_c P\left(T_w - T_{aw}\right) dx + \dot{w}q$$

Expanding and neglecting second-order terms gives

$$\dot{w}\,dh + \dot{w}V\,dV + h\,d\dot{w} + \frac{V^2\,d\dot{w}}{2} - h_{inj}\,d\dot{w} - \frac{V_{inj}^2\,d\dot{w}}{2} = h_c P\,(T_w - T_{aw})\,dx + \dot{w}q$$

Grouping terms gives

$$\dot{w}\,dh + \dot{w}V\,dV + (h - h_{inj})d\dot{w} + \left(\frac{V^2}{2} - \frac{V_{inj}^2}{2}\right)d\dot{w} = h_c P\,(T_w - T_{aw})\,dx + \dot{w}q$$

Substituting $h = C_pT$ and $V = \dot{w}Rg_cT/pA$ gives

$$\dot{w}C_p\,dT + \frac{\dot{w}^2Rg_cT}{pA}\,d\left(\frac{\dot{w}Rg_cT}{pA}\right) + \left(C_pT - C_{p,\mathrm{inj}}T_{\mathrm{inj}} + \frac{\dot{w}^2R^2g_c^2T^2}{2p^2A^2} - \frac{V_{\mathrm{inj}}^2}{2}\right)d\dot{w} = h_cP\left(T_w - T_{\mathrm{aw}}\right)dx + \dot{w}q$$

Dividing by dx yields

$$\dot{w}C_p\frac{dT}{dx} + \frac{\dot{w}^2Rg_cT}{pA}\frac{d}{dx}\left(\frac{\dot{w}Rg_cT}{pA}\right) + \left(C_pT - C_{p,\mathrm{inj}}T_{\mathrm{inj}} + \frac{\dot{w}^2R^2g_c^2T^2}{2p^2A^2} - \frac{V_{\mathrm{inj}}^2}{2}\right)\frac{d\dot{w}}{dx} = h_cP\left(T_w - T_{\mathrm{aw}}\right) + \frac{\dot{w}q}{dx} \qquad \text{(E1)}$$

Expanding the second term gives

$$\frac{d}{dx}\left(\frac{\dot{w}Rg_cT}{pA}\right) = \frac{Rg_cT}{pA}\frac{d\dot{w}}{dx} + \frac{\dot{w}Rg_c}{pA}\frac{dT}{dx} - \frac{\dot{w}Rg_cT}{p^2A}\frac{dp}{dx} - \frac{\dot{w}Rg_cT}{pA^2}\frac{dA}{dx}$$

Solving equation (E1) for dT/dx yields

$$\left(\dot{w}C_p + \frac{\dot{w}^3R^2g_c^2T}{p^2A^2}\right)\frac{dT}{dx} = \left(-C_pT + C_{p,\mathrm{inj}}T_{\mathrm{inj}} - \frac{\dot{w}^2R^2g_c^2T^2}{2p^2A^2} + \frac{V_{\mathrm{inj}}^2}{2} - \frac{\dot{w}^2R^2g_c^2T^2}{p^2A^2}\right)\frac{d\dot{w}}{dx} + \frac{\dot{w}^3R^2g_c^2T^2}{p^3A^2}\frac{dp}{dx} + \frac{\dot{w}^3R^2g_c^2T^2}{p^2A^3}\frac{dA}{dx} + h_cP\left(T_w - T_{\mathrm{aw}}\right) + \frac{\dot{w}q}{dx}$$

Dividing by $\dot{w}C_p$ and substituting $P = 4A/D_h$ gives

$$\left(1 + \frac{\dot{w}^2R^2g_c^2T}{p^2A^2C_p}\right)\frac{dT}{dx} = \left(-\frac{T}{\dot{w}} + \frac{C_{p,\mathrm{inj}}T_{\mathrm{inj}}}{C_p\dot{w}} - \frac{\dot{w}R^2g_c^2T^2}{2C_pp^2A^2} + \frac{V_{\mathrm{inj}}^2}{2C_p\dot{w}} - \frac{\dot{w}R^2g_c^2T^2}{C_pp^2A^2}\right)\frac{d\dot{w}}{dx} + \frac{\dot{w}^2R^2g_c^2T^2}{C_pp^3A^2}\frac{dp}{dx} + \frac{\dot{w}^2R^2g_c^2T^2}{C_pp^2A^3}\frac{dA}{dx} + \frac{h_c4A(T_w - T_{\mathrm{aw}})}{C_p\dot{w}D_h} + \frac{q}{C_p\,dx}$$

From the momentum equation

$$\frac{dp}{dx} = \frac{\left[-\frac{2\left(\frac{\dot{w}}{A}\right)Rg_cT}{pA} + \frac{V_{\mathrm{inj}}}{A}\right]\frac{d\dot{w}}{dx} - \frac{\left(\frac{\dot{w}}{A}\right)^2Rg_c}{p}\frac{dT}{dx} + \frac{\left(\frac{\dot{w}}{A}\right)^2Rg_cT}{pA}\frac{dA}{dx} - \frac{4fRg_cT\left(\frac{\dot{w}}{A}\right)^2}{2pD_h} + \frac{N^2rp}{Rg_cT}\frac{dr}{dx}}{1 - \frac{\left(\frac{\dot{w}}{A}\right)^2Rg_cT}{p^2}}$$

From the energy equation

$$\frac{dT}{dx} = \frac{\left[-\frac{T}{\dot{w}} + \frac{C_{p,\mathrm{inj}}T_{\mathrm{inj}}}{C_p\dot{w}} - \frac{\dot{w}}{2C_p}\left(\frac{Rg_cT}{pA}\right)^2 + \frac{V_{\mathrm{inj}}^2}{2C_p\dot{w}} - \frac{\dot{w}}{C_p}\left(\frac{Rg_cT}{pA}\right)^2\right]\frac{d\dot{w}}{dx} + \frac{1}{C_pp}\left(\frac{\dot{w}Rg_cT}{pA}\right)^2\frac{dp}{dx} + \frac{1}{C_pA}\left(\frac{\dot{w}Rg_cT}{pA}\right)^2\frac{dA}{dx} + \frac{h_c4A(T_w - T_{\mathrm{aw}})}{C_p\dot{w}D_h} + \frac{q}{C_p\,dx}}{1 + \frac{\left(\frac{\dot{w}}{A}\right)^2R^2g_c^2T}{p^2C_p}}$$

Substituting dT/dx into dp/dx gives

$$\frac{dp}{dx} = \frac{1}{C2}\left(\left\{C1\left[\frac{3\dot{w}}{2C_p}\left(\frac{Rg_cT}{pA}\right)^2 + \frac{T}{\dot{w}} - \frac{C_{p,\mathrm{inj}}T_{\mathrm{inj}}}{C_p\dot{w}} - \frac{V_{\mathrm{inj}}^2}{2\dot{w}C_p}\right] + \frac{V_{\mathrm{inj}}}{A} - \frac{2\left(\frac{\dot{w}}{A}\right)Rg_cT}{pA}\right\}\frac{d\dot{w}}{dx}$$

$$+\left[\frac{\left(\frac{\dot{w}}{A}\right)^2 Rg_cT}{pA} - \frac{C1}{C_pA}\left(\frac{\dot{w}Rg_cT}{pA}\right)^2\right]\frac{dA}{dx}$$

$$-\frac{2fRg_cT\left(\frac{\dot{w}}{A}\right)^2}{pD_h} + \frac{N^2rp}{Rg_cT}\frac{dr}{dx}$$

$$-\frac{4h_c(T_w - T_{\mathrm{aw}})C1}{\dot{w}C_pD_h} - \frac{C1q}{C_p\,dx}\Bigg)$$

where

$$C1 = \frac{\left(\frac{\dot{w}}{A}\right)^2 Rg_c}{p\left[1 + \frac{\left(\frac{\dot{w}}{A}\right)^2 R^2g_c^2T}{p^2C_p}\right]}$$

$$C2 = 1 - \frac{\left(\frac{\dot{w}}{A}\right)^2 Rg_cT}{p^2} + \frac{C1}{pC_p}\left(\frac{\dot{w}Rg_cT}{pA}\right)^2$$

This value of dp/dx is then substituted into the energy equation to give dT/dx. The solution is then marched from node to node as described in the main text.

Example Problem

The example given here is a reworked and expanded example 3 from the main text. It is the Rayleigh line flow problem, which could not be solved directly with the original code. It involves adding heat (1329.288 kJ/kg) between stations 1 and 2 and subtracting the same amount of heat between stations 2 and 3. In the main text only heat addition is shown. This example doubles the length of the duct, demonstrates that heat subtraction is also allowed by the code, and shows how closely the end solution matches the input conditions when an equal amount of heat is added and subtracted. For this example equal numbers of slices were used for the heated interval (station 1 to 2) and the cooled interval (station 2 to 3) shown in the following sketch:

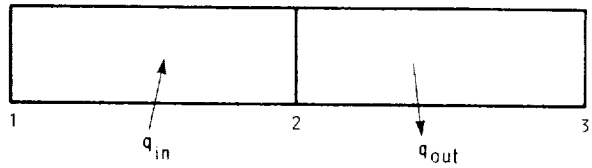

INTERVAL 2-3 IS A MIRROR IMAGE OF INTERVAL 1-2

The problem can be stated as follows:

$$q_{\mathrm{in}} = -q_{\mathrm{out}}$$

The intervals are of equal length and diameter. Begin with set initial conditions: P_{01}, T_{01}, A, γ, D, $\dot{w}$, and M_1. Add heat, $q_{\mathrm{in}} = 1\ 329\ 288$ J/kg, between station 1 and station 2. Take away heat, $q_{\mathrm{out}} = -q_{\mathrm{in}}$, between station 2 and station 3 to see if this gives (within computational error) the original input values.

From Shapiro (ref. 15) the closed-form solution is as follows:

Solve for T_{02}:

$$q_{\mathrm{in}} = C_p(T_{02} - T_{01})$$

Iterate for M_2:

$$\frac{T_{02}}{T_{01}} = \frac{M_2^2}{M_1^2}\frac{\left(1 + \gamma M_1^2\right)^2}{\left(1 + \gamma M_2^2\right)^2}\frac{1 + \frac{\gamma - 1}{2}M_2^2}{1 + \frac{\gamma - 1}{2}M_1^2}$$

Solve for p_2, p_{02}, and T_2:

$$\frac{p_2}{p_1} = \frac{1 + \gamma M_1^2}{1 + \gamma M_2^2}$$

$$\frac{p_{02}}{p_{01}} = \frac{p_2}{p_1}\frac{\left(1 + \frac{\gamma - 1}{2}M_2^2\right)^{\gamma/(\gamma-1)}}{\left(1 + \frac{\gamma - 1}{2}M_1^2\right)^{\gamma/(\gamma-1)}}$$

$$\frac{T_2}{T_1} = \frac{M_2^2}{M_1^2}\frac{\left(1 + \gamma M_1^2\right)^2}{\left(1 + \gamma M_2^2\right)^2}$$

Results are shown in table E-I for 50, 100, and 125 slices in each interval. Improvement is evident between 50 and 100 slices, but between 100 and 125 slices improvement is so slight that additional slices cannot be justified.

TABLE E-I.—COMPARISON OF RESULTS

(a) Heating in a duct

Conditions at duct midpoint	Closed form	50 Slices	100 Slices	125 Slices
T_2'	1625	1625	1625	1625
T_2	1461	1461	1461	1461
p_2'	83.44	83.44	83.44	83.44
p_2	57.45	57.48	57.47	57.47
M_2	0.750	0.7496	0.7497	0.7497

(b) Cooling in a duct

Conditions in duct exit	Closed form	50 Slices	100 Slices	125 Slices
T_3'	300	300	299.9	299.9
T_3	297.6	297.6	297.5	297.5
p_3'	100	99.99	99.99	99.99
p_3	97.25	97.24	97.24	97.24
M_3	0.2000	0.2000	0.2000	0.2000

The input and output for the example problem are as follows:

```
    EXAMPLE PROBLEM 2 HEAT GENERATION - SI UNITS
&DATT IECHO=0, IUNITS=1, IOPPRP=0, RG=287.0, RPM=0.0,
G=1.40, CP=0.23978, XMU=1.8E-4, XK=0.6E-4,
NI=2, ZIN=0.0, RIN=0.0, YIN=0.0, AIN=10., DHIN=3.56825,
IOPTW=0, WIN=.787355,
PTSP=100., TTSP=300., KTIN=0.0,
Z=10.0, 20.0, R=2*0.0, Y=2*0.0, NSLI=2*50, A=2*10., HC=2*0.0,
DH=2*3.56825, F=2*0.00, TW=2*533., Q=1329287.692, -1329287.692 &END
&DATT NSLI=2*100 &END
&DATT NSLI=2*125 &END
```

```
    EXAMPLE PROBLEM 2 HEAT GENERATION - SI UNITS


 SI UNITS

 USER SPECIFIES PHYSICAL PROPERTIES (G, CP, MU AND K)

 COOLANT FLOW RATE IS SPECIFIED

 ROTATIONAL SPEED IS  0.000E+00  RPM

 OUTPUT IN ORIGINAL NODE/INTERVAL FRAME OF REFERENCE
-----------------------------------------------
 INPUT  SLICES  SLICE   SPECIFIED HEAT
  NODE     IN     NO.      IN INTERVAL
  NO.  INTERVAL             (J/KG)
   1       50     50      0.13293E+07
   2       50    100     -0.13293E+07

  I  OPTIONS (IOPT)        Z          R          Y          A          DH          TW          DX          XTOT          KT    NSLI
     FI  HT  FF  CR       (CM)       (CM)       (CM)      (CM**2)     (CM)        (K)         (CM)        (CM)

                      0.0000E+00 0.0000E+00 0.0000E+00 0.1000E+02 0.3568E+01                                      0.0000E+00
  1   0   0   0   0  0.1000E+02 0.0000E+00 0.0000E+00 0.1000E+02 0.3568E+01 0.5330E+03 0.1000E+02 0.1000E+02 0.0000E+00   50
  2   0   0   0   0  0.2000E+02 0.0000E+00 0.0000E+00 0.1000E+02 0.3568E+01 0.5330E+03 0.1000E+02 0.2000E+02 0.0000E+00   50

 I       T          TT          P          PT          W          V          M        GAMMA        CP          VISC.      TH. CNDT.
           (K)        (K)     (N/CM**2)  (N/CM**2)    (KG/S)     (M/S)                        CAL/(GR-K)  GR/(CM-S)  CAL/(CM-S-K)

     0.2976E+03 0.3000E+03 0.9725E+02 0.1000E+03 0.7874E+00 0.6915E+02 0.2000E+00 0.140E+01 0.240E+00 0.180E-03 0.600E-04
  1  0.1461E+04 0.1625E+04 0.5748E+02 0.8344E+02 0.7874E+00 0.5743E+03 0.7496E+00 0.140E+01 0.240E+00 0.180E-03 0.600E-04
  2  0.2976E+03 0.3000E+03 0.9724E+02 0.9999E+02 0.7874E+00 0.6915E+02 0.2000E+00 0.140E+01 0.240E+00 0.180E-03 0.600E-04

        RE          PR          ST          NU          F          FCOR          HC          HCCOR       HCCORC      NTACOR        TAW
                                                                           (CAL/CM**2-S-K)                                          (K)

  1  0.1561E+07 0.7194E+00 0.0000E+00 0.0000E+00 0.0000E+00 0.1000E+01 0.0000E+00  1.0000     1.0000     1.0000    0.1595E+04
  2  0.1561E+07 0.7194E+00 0.0000E+00 0.0000E+00 0.0000E+00 0.1000E+01 0.0000E+00  1.0000     1.0000     1.0000    0.3129E+03
```

EXAMPLE PROBLEM 2 HEAT GENERATION - SI UNITS

SI UNITS

USER SPECIFIES PHYSICAL PROPERTIES (G, CP, MU AND K)

COOLANT FLOW RATE IS SPECIFIED

ROTATIONAL SPEED IS 0.000E+00 RPM

OUTPUT IN ORIGINAL NODE/INTERVAL FRAME OF REFERENCE

INPUT NODE NO.	SLICES IN INTERVAL	SLICE NO.	SPECIFIED HEAT IN INTERVAL (J/KG)
1	100	100	0.13293E+07
2	100	200	-0.13293E+07

I	OPTIONS (IOPT) FI	HT	FF	CR	Z (CM)	R (CM)	Y (CM)	A (CM**2)	DH (CM)	TW (K)	DX (CM)	XTOT (CM)	KT	NSLI
					0.0000E+00	0.0000E+00	0.0000E+00	0.1000E+02	0.3568E+01				0.0000E+00	
1	0	0	0	0	0.1000E+02	0.0000E+00	0.0000E+00	0.1000E+02	0.3568E+01	0.5330E+03	0.1000E+02	0.1000E+02	0.0000E+00	100
2	0	0	0	0	0.2000E+02	0.0000E+00	0.0000E+00	0.1000E+02	0.3568E+01	0.5330E+03	0.1000E+02	0.2000E+02	0.0000E+00	100

I	T (K)	TT (K)	P (N/CM**2)	PT (N/CM**2)	W (KG/S)	V (M/S)	M	GAMMA	CP CAL/(GR-K)	VISC. GR/(CM-S)	TH. CNDT. CAL/(CM-S-K)
	0.2976E+03	0.3000E+03	0.9725E+02	0.1000E+03	0.7874E+00	0.6915E+02	0.2000E+00	0.140E+01	0.240E+00	0.180E-03	0.600E-04
1	0.1461E+04	0.1625E+04	0.5747E+02	0.8344E+02	0.7874E+00	0.5743E+03	0.7497E+00	0.140E+01	0.240E+00	0.180E-03	0.600E-04
2	0.2975E+03	0.2999E+03	0.9724E+02	0.9999E+02	0.7874E+00	0.6914E+02	0.2000E+00	0.140E+01	0.240E+00	0.180E-03	0.600E-04

I	RE	PR	ST	NU	F	FCOR	HC (CAL/CM**2-S-K)	HCCOR	HCCORC	HTACOR	TAW (K)
1	0.1561E+07	0.7194E+00	0.0000E+00	0.0000E+00	0.0000E+00	0.1000E+01	0.0000E+00	1.0000	1.0000	1.0000	0.1602E+04
2	0.1561E+07	0.7194E+00	0.0000E+00	0.0000E+00	0.0000E+00	0.1000E+01	0.0000E+00	1.0000	1.0000	1.0000	0.3063E+03

EXAMPLE PROBLEM 2 HEAT GENERATION - SI UNITS

SI UNITS

USER SPECIFIES PHYSICAL PROPERTIES (G, CP, MU AND K)

COOLANT FLOW RATE IS SPECIFIED

ROTATIONAL SPEED IS 0.000E+00 RPM

OUTPUT IN ORIGINAL NODE/INTERVAL FRAME OF REFERENCE

INPUT NODE NO.	SLICES IN INTERVAL	SLICE NO.	SPECIFIED HEAT IN INTERVAL (J/KG)
1	125	125	0.13293E+07
2	125	250	-0.13293E+07

I	OPTIONS (IOPT) FI	HT	FF	CR	Z (CM)	R (CM)	Y (CM)	A (CM**2)	DH (CM)	TW (K)	DX (CM)	XTOT (CM)	KT	NSLI
					0.0000E+00	0.0000E+00	0.0000E+00	0.1000E+02	0.3568E+01				0.0000E+00	
1	0	0	0	0	0.1000E+02	0.0000E+00	0.0000E+00	0.1000E+02	0.3568E+01	0.5330E+03	0.1000E+02	0.1000E+02	0.0000E+00	125
2	0	0	0	0	0.2000E+02	0.0000E+00	0.0000E+00	0.1000E+02	0.3568E+01	0.5330E+03	0.9999E+01	0.2000E+02	0.0000E+00	125

I	T (K)	TT (K)	P (N/CM**2)	PT (N/CM**2)	W (KG/S)	V (M/S)	M	GAMMA	CP CAL/(GR-K)	VISC. GR/(CM-S)	TH. CNDT. CAL/(CM-S-K)
	0.2976E+03	0.3000E+03	0.9725E+02	0.1000E+03	0.7874E+00	0.6915E+02	0.2000E+00	0.140E+01	0.240E+00	0.180E-03	0.600E-04
1	0.1461E+04	0.1625E+04	0.5747E+02	0.8344E+02	0.7874E+00	0.5744E+03	0.7497E+00	0.140E+01	0.240E+00	0.180E-03	0.600E-04
2	0.2975E+03	0.2999E+03	0.9724E+02	0.9999E+02	0.7874E+00	0.6914E+02	0.2000E+00	0.140E+01	0.240E+00	0.180E-03	0.600E-04

I	RE	PR	ST	NU	F	FCOR	HC (CAL/CM**2-S-K)	HCCOR	HCCORC	HTACOR	TAW (K)
1	0.1561E+07	0.7194E+00	0.0000E+00	0.0000E+00	0.0000E+00	0.1000E+01	0.0000E+00	1.0000	1.0000	1.0000	0.1603E+04
2	0.1561E+07	0.7194E+00	0.0000E+00	0.0000E+00	0.0000E+00	0.1000E+01	0.0000E+00	1.0000	1.0000	1.0000	0.3049E+03

References

1. Calvert, G.S; and Okapuu, U.: Design and Evaluation of a High-Temperature Radial Turbine—Phase I Final Report. (PWA-FR-2858 USAAVLABS-TR-68-69, Pratt & Whitney Aircraft; Contract number: DAAJ02-68-C0003) Jan. 1969.
2. Vershure, R.W, Jr., et al.: A Cooled Laminated Radial Turbine Technology Demonstration. AIAA Paper 80-0300, Jan. 1980.
3. Ewing, B.A.; Monson, D.S.; and Lane, J.M.: Allison High-Temperature Radial Turbine Demonstration. AIAA Paper 80-0301, Jan. 1980.
4. Hammer, A.N., et al.: Composite Casting/Bonding Construction of an Air-Cooled, High Temperature Radial Turbine Wheel. Advances in Aerospace Propulsion; Proceedings of the Aerospace Congress and Exposition, Society of Automotive Engineers, Warrendale, PA, 1983, pp. 93-99 (also SAE Paper 831519).
5. Kumar, G.N.; Roelke, R.J.; and Meitner, P.L.: A Generalized One Dimensional Computer Code for Turbomachinery Cooling Passage Flow Calculations. AIAA Paper 89-2574, July 1989.
6. Webb, R.L.; Eckert, E.R.; and Goldstein, R.J.: Heat Transfer and Friction in Tubes With Repeated-Rib Roughness. Int. J. Heat Mass Transfer, vol. 14, no. 4, 1971, pp. 601-617.
7. Welty, J.R.; Wicks, C.E.; and Wilson, R.E.: Fundamentals of Momentum, Heat, and Mass Transfer. Second Ed., John Wiley & Sons, 1976.
8. Van Fossen, G.J.: Heat Transfer Coefficients for Staggered Arrays of Short Pin Fins. ASME Paper 81-GT-75, Mar. 1981.
9. Morris, W.D.; and Ayhan, T.: Observations on the Influence of Rotation Heat Transfer in the Coolant Channels of Gas Turbine Rotor Blades. Inst. Mech. Eng. (London) Proc., vol. 193, Sept. 1979, pp. 303-311.
10. Morris, W.D.: Heat Transfer and Fluid Flow in Rotating Coolant Channels. John Wiley & Sons, 1981.
11. Meitner, P.L.; and Hippensteele, S.A.: Experimental Flow Coefficients of a Full-Coverage Film-Cooled-Vane Chamber. NASA TP-1036, 1977.
12. Chupp, R.E., et al.: Evaluation of Internal Heat Transfer Coefficients for Impingement Cooled Turbine Airfoils. AIAA Paper 68-564, June 1968.
13. Kunkle, J.S.; Wilson, S.D.; and Cota, R.A.: Compressed Gas Handbook. NASA SP-3045, 1969.
14. Poferl, D.J.; Svehla, R.A.; and Lewandowski, K.: Thermodynamic and Transport Properties of Air and the Combustion Products of Natural Gas and of ASTM-A-1 Fuel With Air. NASA TN D-5452, 1969.
15. Shapiro, Ascher H.: The Dynamics and Thermodynamics of Compressible Fluid Flow, Volume 1. Ronald Press Co., 1953.

NASA
National Aeronautics and Space Administration

Report Documentation Page

1. Report No.	2. Government Accession No.	3. Recipient's Catalog No.
NASA TP-2985 AVSCOM TR-89-C-008		

4. Title and Subtitle	5. Report Date
Computer Code for Predicting Coolant Flow and Heat Transfer in Turbomachinery	September 1990
	6. Performing Organization Code

7. Author(s)	8. Performing Organization Report No.
Peter L. Meitner	E-5186
	10. Work Unit No. 505-62-0K 1L161102AH45

9. Performing Organization Name and Address	11. Contract or Grant No.
NASA Lewis Research Center Cleveland, Ohio 44135-3191 and Propulsion Directorate U.S. Army Aviation Systems Command Cleveland, Ohio 44135-3191	
	13. Type of Report and Period Covered Technical Paper

12. Sponsoring Agency Name and Address	14. Sponsoring Agency Code
National Aeronautics and Space Administration Washington, D.C. 20546-0001 and U.S. Army Aviation Systems Command St. Louis, Mo. 63120-1798	

15. Supplementary Notes

Peter L. Meitner, Propulsion Directorate, U.S. Army Aviation Systems Command. An added feature of the code that allows direct specification of heat generation is described in appendix E by Teresa R. Kline, Propulsion Directorate, U.S. Army Aviation Systems Command.

16. Abstract

A computer code was developed to analyze any turbomachinery coolant flow path geometry that consists of a single flow passage with a unique inlet and exit. Flow can be bled off for tip-cap impingement cooling, and a flow bypass can be specified in which coolant flow is taken off at one point in the flow channel and reintroduced at a point farther downstream in the same channel. The user may either choose the coolant flow rate or let the program determine the flow rate from specified inlet and exit conditions. The computer code integrates the one-dimensional momentum and energy equations along a defined flow path and calculates the coolant's flow rate, temperature, pressure, and velocity and the heat transfer coefficients along the passage. The equations account for area change, mass addition or subtraction, pumping, friction, and heat transfer.

17. Key Words (Suggested by Author(s))	18. Distribution Statement
Turbine cooling Internal heat transfer Radial turbine Axial turbine	Unclassified – Unlimited Subject Category 07

19. Security Classif. (of this report)	20. Security Classif. (of this page)	21. No. of pages	22. Price*
Unclassified	Unclassified	41	A03

*For sale by the National Technical Information Service, Springfield, Virginia 22161

NASA-Langley, 1990